COPY NO. 18

UNITED AIRCRAFT CORPORATION
RESEARCH LABORATORIES
EAST HARTFORD, CONN.

A-920057-5

Research on the Collision Probabilities of Electrons and Cesium Ions in Cesium Vapor

Final Report
May 1, 1962 through May 31, 1963
Contract No. NASr-112

REPORTED BY R. H. Bullis
R. H. Bullis

R. K. Flavin
R. K. Flavin

APPROVED BY R. G. Meyerand, Jr.
R. G. Meyerand, Jr.
Principal Scientist
Plasma Physics

NO. OF PAGES 49

DATE May 31, 1963

Report A-920057-5

Research on the Collision Probabilities of Electrons and Cesium Ions in Cesium Vapor

TABLE OF CONTENTS

Report A-920057-5

Research on the Collision Probabilities of Electrons and Cesium Ions in Cesium Vapor

Final Report

Contract No. NASr-112

SUMMARY

The collision cross sections of ions and electrons in cesium vapor were determined by an experimental research investigation conducted at the United Aircraft Corporation Research Laboratories during the period May 1, 1962 through May 31, 1963. Values for these cross sections permit the formulation of a quantitative analysis of the operation of thermionic converters or other devices employing cesium vapor in an ionized state. Electron cyclotron resonance techniques were employed to determine the electron collision cross sections and a modification of the Ramsauer experiment designed to eliminate contact potentials was employed to determine the ion collision cross sections. The collision cross sections for electrons with cesium atoms were determined to vary from 1150 to 1500 P_c (collisions per centimeter at one millimeter gas pressure) at energies of 0.05 and 0.10 ev, respectively, with a maximum cross section of 1900 P_c at .065 ev. The collision cross sections of ions with cesium atoms were determined to vary from 5,685 to 25,570 P_c at energies of 9.7 to 0.12 ev respectively.

RECOMMENDATIONS

Further research work on the determination of the collision cross section of electrons with cesium atoms should include additional studies of the electron energy distribution in cesium vapor under conditions of thermal ionization and of non-equilibrium ionization produced by rf excitation. Such an investigation would provide additional information on the velocity dependence of the cross section in the transition regime at electron energies less than 0.065 ev at which energies thermal ionization was employed in the present experiments. In addition, these studies would provide an improved understanding of the mechanisms associated with non-equilibrium ionization phenomena. Measurements of electron-atom collision cross sections in the energy range above 0.1 ev

would be extremely valuable since the effect on the measured collision cross sections of higher energy electrons in the thermal distribution at energies below 0.1 ev could be properly considered.

Experimental studies should be undertaken to determine ion-atom collision cross sections at energies below 0.1 ev in order to obtain ion cross-section data for an energy range of importance to thermionic converter performance. Also such studies would permit the fundamental limit of the experimental technique used in the present investigation to be determined. In addition, studies should be undertaken to determine the effect on the cross section of the thermal velocity of the atoms in the collision chamber so that their energy contribution to the collision can be properly considered at very low energies. The present experimental apparatus with relatively little modification could be used to determine the ion collision cross sections in an energy range from 0.1 to 10 ev of other alkali metals, such as sodium, potassium, and rubidium. These latter studies would provide important data pertaining to MHD flows and other applications.

INTRODUCTION

In order to permit the formulation of a quantitative analysis of the operation of thermionic converters or other devices employing cesium vapor in an ionized state, an experimental research investigation was undertaken at the UAC Research Laboratories under the sponsorship of the National Aeronautics and Space Administration to determine the collision cross sections of ions and electrons in cesium vapor. The research program was divided into two main parts: the measurements of the total collision cross section of cesium ions with cesium atoms in the energy range of 0.1 to 10 ev and the measurement of the collision cross section of electrons with cesium atoms in the energy range of 0.05 to 0.10 ev.

GENERAL DISCUSSION OF EXPERIMENTAL METHODS AND DATA ANALYSIS

The electron cyclotron resonance techniques which were employed to determine the electron collision cross sections are based on the physical principal that the resonant frequency of free electrons gyrating in a magnetic field is broadened by collisions with gas atoms. The collision frequency between electrons and atoms can be measured, therefore, by determining the width of the cyclotron resonance line. An extremely sensitive microwave spectrometer which was constructed to attain accurate measurements of the cyclotron resonance line shape incorporated an electromagnet with a very homogeneous magnetic field region and time modulation of the field so that phase-sensitive detection could be used. The microwave circuitry included a balanced mixer-detector with an extremely low noise figure so that microwave powers of the order of 10^{-16} watts could be detected. The output from the microwave circuitry was phase-sensitively detected and displayed on x-y plots. The temperature of the cesium was controlled by an oven and Tophet A heating strips adjacent to the cesium tube.

The data obtained were analyzed using the detailed line shape of the cyclotron resonance to predict not only the absolute magnitude of the collision cross section but also the dependence of the cross section on the electron velocity. A new representation for the collision frequency incorporating two terms to predict more accurately the velocity dependence was employed in these calculations rather than the normal single term approximation which has been used in the past for microwave

experiments. At the higher energies, ionization of the cesium by external rf power was not required and the thermal ionization due to the temperature of the cesium gas alone produced free electrons in sufficient density to produce detectable cyclotron spectra. When thermal energy alone is used to generate free electrons, the electron energy distribution must necessarily be Maxwellian which makes the interpretation of the spectra unique. This phemonenon has not been observed in any other experiments reported to date and represents a significant advance in the state of the art of collision cross-section measurement techniques.

A modification of the Ramsauer experiment designed to eliminate contact potentials was employed to measure the ion collision cross sections. In this modification, the measurement of the ion-atom cross section was accomplished by measuring the attentuation of a beam of cesium ions as it passes through cesium vapor. The collisions occur in the presence of a magnetic field which not only accomplishes an energy analysis of the ions, but removes ions which have suffered energy degrading collisions. The elimination of contact potentials was accomplished by employing a specially designed collision chamber fabricated with re-entrance slits so that any electric fields generated external to the chamber do not penetrate into it. Therefore, if an ion passes through the chamber, its energy is known during the time it is in the chamber and is colliding with atoms. The chamber was constructed of extremely pure, homogeneous copper which was electroformed into the desired shape to provide a region free of contact and thermoelectric potentials. This arrangement is necessary for accurate experimental measurements of collision cross sections at low energies. The cesium ion source employed a porous tungsten disk through which cesium was passed and ions were generated on the high work function tungsten surface. The beam was focused by a succession of slits and was decelerated to a very low energy. Upon emergence from the collision chamber, the beam was collected either by a Faraday cup or a 20-stage electron multiplier. The gain of the multiplier was sufficiently high to permit currents as low as 10^{-18} amps to be measured. The entire vacuum system was constructed of stainless steel and was baked out to remove impurities from the system.

A detailed description of the experimental research work to determine the collision cross section of ions and electrons is presented in the subsequent sections of this report.

ELECTRON COLLISION CROSS SECTION MEASUREMENT

Introduction

Electron-atom collisions play the dominant role in determining transport phenomena in partially ionized plasmas. The electrical conductivity in a low temperature non-equilibrium cesium plasma is determined almost wholly by the collision cross section of electrons with atoms. Accurate data for this collision cross section is extremely important for a fundamental understanding of the behavior of any device such as thermionic converters using cesium vapor in this partially ionized state. Electron energies of most interest in such devices are in the vicinity of 0.1 ev. Accurate data in this energy range is not available in the literature. Low electron energies rule out the use of beam cross-section measurement techniques such as Ramsauer experiments.

The most versatile and accurate methods for the determination of low-energy collision cross sections are microwave techniques. The electron cyclotron resonance microwave technique (Refs. 1,2 & 3) has the additional advantage of high sensitivity thus allowing accurate measurements at very low electron densities. For this reason only a very small percentage of the cesium vapor need be ionized to make the collision cross section measurement; consequently, cesium reactions with container walls are minimized. In addition, electron-ion collision cross sections are quite large at these low energies, making it important to keep the percentage ionization in the plasma very low. Also, the high sensitivity of the technique allows the very low electron densities associated with thermal ionization to be used to make collision cross-section measurements. With only heat as the energy input to the plasma, a Maxwellian electron energy distribution is assured, thus increasing the confidence in the measurements.

In essence the electron cyclotron resonance technique requires only the measurement of frequency or conversely magnetic field (which may be converted to frequency through various nuclear and atomic resonance phenomena) to determine the collision cross section, and does not involve absolute measurements of the collection efficiency of electrodes, etc. In addition, the electron cyclotron resonance method has advantages over conventional microwave techniques in that the microwave interaction is highly dispersive in a relatively narrow frequency range, and the spectral line shape of the interaction is a function of the dependence of the collision frequency on electron velocity. Therefore, information on

the velocity dependence of the collision cross section may be obtained at a single electron temperature.

Physical Model and Experimental Limitations

The motion of an electron in a combined ac electric field and dc magnetic field lends itself to a simplified determination of the electron collision cross section. When the cyclotron frequency of the electron in a magnetic field is equal to the frequency of the applied or detected microwave electric field, the electrons will absorb or radiate power and the line shape of this absorption or radiation is related to the collision frequency. In the absence of collisions an electron in a dc magnetic field will radiate a monochromatic frequency given by eB/m. However, damping or collisions will broaden this spectrum and will provide a means for determining the electron collision frequency by measuring the widths of the resonance line.

Other effects, however, may also produce broadening of the line. Doppler shifts due to the fact that the electron may be traveling toward or away from the direction of observation can produce significant broadening of the radiation. However, Doppler broadening is small compared to pressure broadening when the ratio of the collision frequency to the frequency of the microwave signal is large compared to the ratio of the electron velocity to the velocity of light. Doppler broadening essentially represents an upper limit to the electron temperatures that can be utilized in this technique but for energies of interest to conventional plasma devices, this restriction is not important. In addition, transit time effects may broaden the line. An electron moving through the region that is sensing the absorbed or radiated microwave power will emit a finite length wave train during the time of interaction and this wave train will contain harmonics which will broaden the line. Once again, the amount of broadening due to transit time effects is related to the electron energy as the electron velocity will determine the time duration of the interaction. Transit time effects are also small with regard to the broadening produced by collisions in the energy range of interest.

Stark effect due to the presence of many positively charged ions which would randomly accelerate the electrons, could also broaden the resonance line. However, for sufficiently low plasma densities which are always used in these experiments, the Stark effect will not produce appreciable broadening.

Inhomogeneities in the dc magnetic field will change the value of the cyclotron frequency of the electrons. Therefore, particular attention must be paid to the question of magnetic field homogeneity and values less than one part in a thousand must be maintained over the plasma volume if the subsequent line broadening is to be reduced to an acceptable value.

The electromagnetic energy that is radiated or absorbed by the electrons will be affected by the dielectric constant of the plasma in which the electrons are moving. The dielectric constant of the plasma differs only slightly from that of free space for low electron densities which reduces the plasma broadening effects to negligible values. Therefore, if microwave instrumentation in the 10^{10} cycles/sec region is to be used, electron and ion densities below 10^{8} per cm^3 must be maintained in the plasma to obtain meaningful measurements in the pressure range used ($p > 50$ μ Hg).

Microwave Attenuation Coefficient

The development of the Boltzmann equation leading to the tensor dielectric coefficient for a tenuous plasma in a magnetic field follows the work of W. P. Allis[4] and L. Mower.[5] The attenuation coefficient for a plane wave propagating in an infinite homogeneous plasma with the Poynting vector and E-field both perpendicular to the magnetic field is found to be given by

$$\beta = \frac{k_0 e^2}{4m\epsilon_0\omega} \int \frac{4\pi}{3} \frac{df_0^0}{dv} v^3 \left\{ \frac{\nu_c(v)}{\nu_c^2 + (\omega - \omega_b)^2} \right\} dv \qquad (1)$$

where

$k_0 = 2\pi/\lambda$ (λ = free space wavelength)

e = electron charge
m = electron mass
ϵ_0 = permittivity of free space

ω = frequency of E-field

ω_b = electron cyclotron frequency

f_o^o = particle distribution function

ν_c = collision frequency for momentum transfer

This derivation holds in the limit of low electron densities when

$\omega_p^2/\nu_c\,\omega_b << 1$. ($\omega_p \equiv \left[ne^2/m\epsilon_o\right]^{1/2}$ is the plasma radian frequency)

and when the non-resonant term is negligible. We see that this is in the standard Lorentzian form, and when ν_c is not a function of velocity, the half-width is directly related to the collision frequency. For a thermalized plasma in which Kirchhoff's law applies the ratio of the emission to the absorption is a constant. Therefore, the line structure of the cyclotron radiation spectra is identical to the absorption spectra.

The line shape of a cyclotron resonance absorption spectra is the only consideration in the determination of the collision frequency for momentum transfer. For this reason the free space analysis of the propagation constant can be applied to a bounded plasma in a waveguide if the effective dielectric constant is very slightly different from that of free space (low electron densities) and the electric field is sufficiently low so that the electrons are not heated during the measurement. For waveguide propagation the term outside the integral in Eq. 1 is then a constant representing an average over the waveguide cross section.

In microwave spectroscopy the absorption spectra are usually displayed in derivative form. For a Maxwellian distribution of velocities the derivative of the attenuation coefficient is given by

$$\frac{d\beta}{dX} \approx X \int_0^\infty v^4 e^{-av^2} \left\{ \frac{\nu_c(v)}{\left[\nu_c^2 + X^2\right]^2} \right\} dv \qquad (2)$$

where $X = (\omega - \omega_b)$ and $a = \frac{m}{2kT}$

Case of Non-constant Collision Frequency

Let us assume that the velocity dependence of the collision frequency can be approximated by the relation

$$\nu\,(v) = A + Bv^{h} \tag{3}$$

where A, B, and h are constants.

Substituting into Eq. 2 we find the derivative of the absorption coefficient is given by

$$\frac{d\beta}{dX} \approx C\int_{0}^{\infty} y^{3/2} e^{-y} \left\{ \frac{\gamma + y^{\ell}}{\left[(\gamma + y^{\ell})^{2} + C^{2}\right]^{2}} \right\} dy \tag{4}$$

where $y = av^{2}$, $h = 2\ell$, $\gamma = \frac{A}{B} a^{\ell}$, and $c = \frac{X}{B} a^{\ell}$

This integral has been programmed on a computer for $0 \leq h \leq 3$, and $\gamma^{2} = 0, 0.01, 0.1$, and 1.0. Before discussing the results, it would be well to define the " Ω " width of a spectrum in derivative form. A typical absorption spectrum is illustrated in Fig. 1A. One half of this spectrum is drawn in Fig. 1B with the peak normalized to one. The " Ω " width refers to the width taken at the fraction Ω of the peak value where the width extends from $|\omega - \omega_{b}| = 0$ to the wing of the spectrum.

The solutions of the integral in Eq. 4 are shown in Fig. 2. where the subscript Ω refers to the widths just described. If γ, h and X_{Ω} are measured experimentally, then the collision frequency is determined by the equation

$$\nu_{c}(v) = \frac{X_{\Omega}}{C_{\Omega}} (\gamma + a^{\ell} v^{2\ell}) \tag{5}$$

For the assumption $\nu_{c}(v) = A + Bv^{h}$ to be valid the relation $X_{\Omega}/X_{I} = C_{\Omega}/C_{I}$ must hold for any width Ω. Figure 3 shows the results of the theoretical ratios of the spectral line widths for three values of γ^{2}. One might then determine γ and h experimentally from a single spectra by measuring X_{Ω}/X_{I} and obtaining the best consistent "fit" for various Ω.

Experiment

The geometry employed in the collision cross section measurement is shown in Fig. 4. Electrons are allowed to drift along a dc magnetic field into a measurement cell contained within a piece of x-band (9375 mc) waveguide. The electrons are supplied by an ac breakdown of the gas external to the measurement cell when the ambient temperature of the cesium vapor is less than 750 K. With the present sensitivity of the microwave spectrometer used to monitor the cyclotron resonance absorption there are sufficient electrons in thermal equilibrium with the cesium vapor at temperatures above 750 K to eliminate the need for an external electron source. The Saha equation for ionization equilibrium in cesium vapor at a pressure of 100 microns Hg, sets this minimum detectable electron density at approximately 10^4 electrons/cm^3.

If the electron source is external to the measurement cell the electrons will lose energy in collisions with the gas atoms and thermalize as they random walk into the cell. In this way a source of low energy electrons is provided in the waveguide and their energy can be controlled by regulating the ambient temperature of the cell body. The collision cross section of the electrons can then be determined by observing the spectral shape of the cyclotron resonance absorption of a probing microwave signal.

The experimental apparatus consists of a 12-inch pole piece electromagnet with a highly regulated power supply, a microwave spectrometer, and the cesium tube with its oven housing.

To eliminate line broadening effects due to magnetic field inhomogeneities an electro-magnet with a 12-inch dia. pole piece was used and a 1-1/2 inch wide iron ring was added to increase the effective pole face diameter to 15 inches. The air gap is 9-1/2 inches to accomodate a double oven assembly which will control the cesium pressure in the measurement cell. The magnet power supply is current regulated to one part in 10^5 by a feed-back system incorporating a reference cell. The magnetic field in the gap was measured with NMR equipment and found to be homogenous to 1 part in 10^3 at a magnetic field of 3350 gauss over a cylinder 1 cm in diameter x 2 cm in length in the center of the air gap which is a volume in excess of the plasma volume employed in the experiment.

Illustrated in Fig. 5 is a block diagram of the X-band microwave spectrometer which was used to monitor and display the cyclotron resonance power absorption. The probe klystron is stabilized in frequency by inducing a very small 90 kc frequency modulation on the klystron output. By sampling the reflections from a reference cavity with a phase detector, an error signal can be derived which, if applied with

the correct polarity to the reflector electrode, stabilizes the klystron frequency to correspond to the resonant frequency of the reference cavity. In this way the probe klystron was stabilized to 1 part in 10^7 over a period of one hour. The local oscillator klystron is also stabilized in frequency by mixing the output with that of the probe klystron and feeding the difference frequency to a 30 mc discriminator. Again, if the correct polarity is applied to the L.O. klystron reflector, the frequency output will be stabilized at 30 mc difference from the probe frequency. This stability is very important in reducing the overall noise figure of the spectrometer since the superheterodyne receiver is a high gain 30 mc amplifier which has a very narrow bandwidth. The receiver incorporated IN23F silicon diodes in a balanced crystal mixer matched to an L.E.L. 30 mc, 120 db I.F. strip with a 1 mc bandwidth for an overall noise figure of less than 7 db and a sensitivity of approximately 10^{-16} watts.

The microwave spectrometer can be used either as a bridge circuit for maximum sensitivity, or, for ease of operation, as a straight transmission geometry. The usual technique of unbalancing the bridge slightly in amplitude but not in phase eliminates the dispersion effects which occur simultaneously with absorption. For the straight transmission geometry this is accomplished by properly matching the detector to the waveguide.

The fact that reflections from the plasma are important was discussed in length in Appendix I to Quarterly Status Report No. 1 UAC Research Labs A-920057-1. To eliminate the error introduced by reflections from the plasma, which is appreciable in the wings of the spectra, the microwave probe signal is fed through a 20 db directional coupler with 40 db directivity as illustrated in the block diagram. An adjustable short is placed on the end of the directional coupler away from the measurement cell. The short is used to reflect power lost to the transmitted wave by reflections at the plasma. If the reflections at the short are adjusted to have the correct phase, the power reflected by the plasma will add once again to the transmitted wave and the only power loss detected by the receiver will be that due to real absorption in the plasma.

A 500 cycle audio oscillator and power amplifier are used to drive the modulation coils on the sides of the measurement cell. The oscillator also provides a reference signal for the phase detector which is described by D. J. E. Ingram[6]. The output from the phase detector is then fed to a high impedance dc amplifier and displayed on an X-Y recorder. An electronic sweep circuit drives the magnet power supply to provide sweep amplitudes up to 1000 gauss in sweep times up to 15 minutes. The slow sweep speeds allow time constants up to 10 sec to be incorporated into the output of the phase detector for maximum sensitivity and discrimination against random noise. A

voltage derived from a precision resistor in series with the electromagnet is used to drive the X-axis of the X-Y recorder. Properly calibrated this voltage is directly related to the magnetic field strength and therefore to the electron cyclotron frequency.

In order to be able to interpret the absorption spectra a calibration of the detection instrumentation was performed. The microwave input power level was adjusted so that the balanced crystal detector represented pure square-law detection. This level is approximately 10^{-7} watts which is sufficiently low to neglect plasma heating during the microwave measurement. The ferrite modulator is used to simulate the effect of audio modulating the dc magnetic field. In this way the entire spectrometer can be calibrated for linearity of response.

The double oven housing the cesium measurement cell and plasma drift tube is pictured in Fig. 6. The initial tubes were fabricated of quartz. To investigate the possibility of cesium reactions with the tube walls at high temperatures, the last tube was constructed of G. E. Lucalox (Al_2O_3) ceramic in the waveguide region. After bake out a vacuum of 10^{-8} mm Hg was obtained before admitting the cesium which was assayed at 99.9 per cent purity. The portion containing the cesium ampule is located in the lower oven. The upper part of the tube includes a 7 mm o.d. straight quartz section 12 cm long which is directed along the axis of the magnet pole pieces. The distance between the region of the breakdown and the waveguide is sufficiently long so that the electrons will suffer enough collisions to thermalize at the temperature of the vapor before entering the waveguide. The stainless steel waveguide measurement cell situated exactly in the center of the magnet air gap contains two one-inch tubular projections from the narrow wall which represent waveguide beyond cutoff to the microwave signal. The quartz drift tube passes through the waveguide so as to fill most of the waveguide cross section. Situated at the start of the quartz drift tube is a breakdown coil wound on a boron nitride coil form and connected to a 600 mc power oscillator. On each side of the waveguide are fastened the two coils which are used to modulate the dc magnetic field in the waveguide at 500 cycles/sec. Not shown in the diagram are the temperature control heaters and temperature sensing components which are used as part of an oven temperature regulator circuit. In operation this circuit is capable of stabilizing the oven temperature to $\pm$ 0.5 F at 500 F. This control is exceedingly important in view of the fact that for cesium vapor pressures in the range of 100-500 μ Hg the pressure will change approximately 5-10 μ Hg/F. The upper oven temperature is always maintained at a higher value than the temperature of the lower oven to prevent the possibility of cesium condensing on the walls of the drift tube. The double oven assembly also allows one to independently control the pressure in the system by regulating the

lower temperature and to control the electron energy by regulating the upper oven temperature. The oven was designed to operate at the maximum temperature of 800 K.

In order to increase the ambient temperature of the measurement cell to 1150 K a local resistive heating technique was used which is depicted in Fig. 7. Two Tophet A ribbons 1/8 inch wide were inserted between the cesium tube and a concentric 8 mm i.d. quartz tube such that they are diametrically opposite and oriented for a minimum perturbation of the microwave electric field. The ribbons are connected in series and heated with a regulated dc power supply. Approximately 350 watts of power was needed to bring the cesium tube up to 1150 K which corresponds to an electron energy of 0.10 ev.

Experimental Results

To determine the effect of various experimental parameters, the line shape was first determined as a function of the rf field strength in the waveguide. At high microwave probing levels, the electron energy can be perturbed and errors may be introduced in the determination of the collision frequency due to the fact that the electrons are at an elevated temperature. However, for low microwave power levels, the line shape is unaffected by the strength of the microwave power signals as is shown in Fig. 8. The power level was carefully controlled throughout all the experiments to make certain that line broadening due to microwave probing was negligible.

Excessive modulation of the dc magnetic field will also give a broadened line shape as is shown in Fig. 9. The half width of the spectrum is plotted as a function of the intensity of the ac modulating field. Once again, it should be noted that for sufficiently low modulating powers broadening of the line does not occur.

To assure that the Tophet A ribbons in the waveguide measurement cell would not affect the detailed line structure of the absorption spectrum, the spectra were carefully compared with previous data taken at the same electron temperature but without the heater ribbons in place. The only noticeable change was a decrease in the overall sensitivity of the spectrometer, while the line shape remained the same.

Since the electron collision frequency is directly proportional to the gas pressure, increasing the cesium pressure should result in the line width increasing linearly as a function of pressure as is shown in Fig. 10. The fact that the line width varies linearly as a function of gas pressure also serves to demonstrate that the electron energy distribution is Maxwellian at the gas temperature. If increasing the gas pressure resulted in a line shape change which was not directly proportional to the gas pressure, then there is evidence that the electrons have not suffered a sufficient number of collisions before entering the measurement cell to thermalize with the gas. Increasing the gas pressure would increase the number of collisions the electrons suffered and the energy distribution would more closely resemble a Maxwellian. Since the relationship between line width and gas pressure is linear, it may be assumed that the electrons have come into thermal equilibrium with the gas.

Analysis of Data

Since the inflection point width is the most accurate section of the spectra to locate, it was used as the standard width to determine the collision cross section. To further increase the accuracy of the measurement, the slope of the inflection point width versus pressure (which was linear in all cases) was used to determine the value of $X_I = |\omega - \omega_b|_I$ which occurs in equation (5). The slope of the inflection point line width versus pressure in gauss/mm Hg, designated $(\frac{\Delta B}{\Delta P})_I$, is related to X_I in the following manner:

$$X_I = |\omega - \omega_b|_I = p(1.76 \times 10^7)(\frac{\Delta B}{\Delta P})_I \tag{6}$$

where p is the pressure in mm Hg.

The collision probability, P_c, defined as the number of collisions per cm path length per mm Hg pressure at 0 C is given by the relation

$$V_c = p_o P_c v \tag{7}$$

where $p_o = 273/T\ p$ is a "reduced" pressure.

Combining equations (5), (6), and (7) we have as an equation for the collision probability in terms of experimental parameters

$$P_c(v) = \frac{(6.44 \times 10^4)(\gamma + a^{h/2} v^h) T}{c_I v} (\frac{\Delta B}{\Delta P})_I \tag{8}$$

The collision probability values obtained in this experiment are plotted in Fig. 11 with the error bars indicating the possible spread in value due to a scatter of points in the vicinity of that energy. It should be pointed out that the data presented here was accumulated with three different cesium tubes: two constructed of quartz, and one with the electron drift section constructed of G.E. Lucalox ceramic.

In order to be consistent with the γ and h values predicted from single spectra, all data taken below 750 K was interpreted as being Lorentzian ($\gamma = h = 0$). Above 750 K, where Saha equilibrium was the condition, the spectra were interpreted with $\gamma = 3$, $h = 1$, again determined from single spectra. It should be pointed out that the velocity dependence predicted from single spectra for the cases of thermal ionization equilibrium agree quite well with the dependence found by changing the cesium temperature.

The cross sections are also shown in Fig. 12 in comparison to the results of many other investigations up to energies of 1.0 ev.

Discussion of Results

The cyclotron resonance absorption technique has proved to be a very sensitive and accurate technique for the determination of low energy electron collision cross sections. The assumption that the spectra are predominantly pressure broadened has been thoroughly demonstrated experimentally giving confidence in the cross-section measurement. In addition, the assumption that the electron distribution function is not only Maxwellian but also in thermal equilibrium with the background gas atoms has been experimentally verified for those measurements where no external electron source was necessary. This last condition is unique for cross-section measurements in this energy range.

The velocity dependence of the collision frequency has been definitely shown to influence the interpretation of spectral widths. For this reason, it is important that the velocity dependence predicted from single spectra be consistent with the variation of spectral widths with ambient temperature changes. This is not the case in our present analysis for data below 750 K where an external electron source by rf breakdown was necessary for the measurement. For this reason more credence should be given to the cross-section values determined under the conditions of Saha equilibrium. Nevertheless, it is felt that the cross-section values at the lower energies are at least accurate to 50 percent, and could become more accurate with further work.

The fact that the transition region between non-equilibrium ionization and thermal equilibrium ionization is available for experimental measurements provides a proper way to ascertain whether or not different electron source configurations do indeed supply thermal electrons for cross-section measurements.

The assumption of viscous gas flow in the presence of a temperature gradient between the upper and lower ovens should be verified to have complete confidence in the values assigned to the absolute pressure in the upper oven.

ACKNOWLEDGEMENTS

The authors would like to gratefully acknowledge the collaboration of Professor J. L. Hirshfield of Yale University, New Haven, Connecticut in the many helpful discussions on both the theoretical and experimental aspects of this experiment.

The help of Mrs. B. Frasca of the United Aircraft Corporation Research Laboratories in obtaining the experimental data and its reduction is also acknowledged.

REFERENCES

1. D. C. Kelley, H. Margenau, and S. C. Brown, Phys. Rev. 108, 1367, (1957).

2. R. M. Hill, Sylvania Technical Report MPL-13 (1958).

3. J. L. Hirshfield and S. C. Brown, Phys. Rev. 122, 719 (1961).

4. W. P. Allis, Handbuch der Physik (Springer Verlag, Berlin 1956), Vol. 21.

5. L. Mower, Sylvania Technical Report MPL-1 (1956).

6. D. J. E. Ingram, Free Radicals as Studied by Electron Spin Resonance, (Academic Press, New York, 1958).

7. R. B. Brode, Phys. Rev., 34, 673 (1929).

8. C. Boeckner and F. L. Mohler, BSJR, 10, 357 (1933).

9. R. K. Steinberg, J. APPL. PHYS., 21, 1028 (1950).

10. G. J. Mullaney and N. R. Dibelius, ARS Journal, P. 1575 (November 1961).

11. N. D. Morgulis and Yu. P. Korchevoi, Zhurnal Tekhnicheskoi Fiziki, Vol. 32, No. 7, pp. 900-902, (July, 1962).

12. C. L. Chen and M. Raether, Phys. Rev., 128, 2679 (1962).

13. D. N. Mirlin, G. E. Pikus, and V. G. Yur'ev, Soviet Phys. - Tech. Phys. Vol 7, 559, (December 1962).

FIG. I

FIG. IA

MICROWAVE POWER ABSORPTION (PHASE DETECTION)

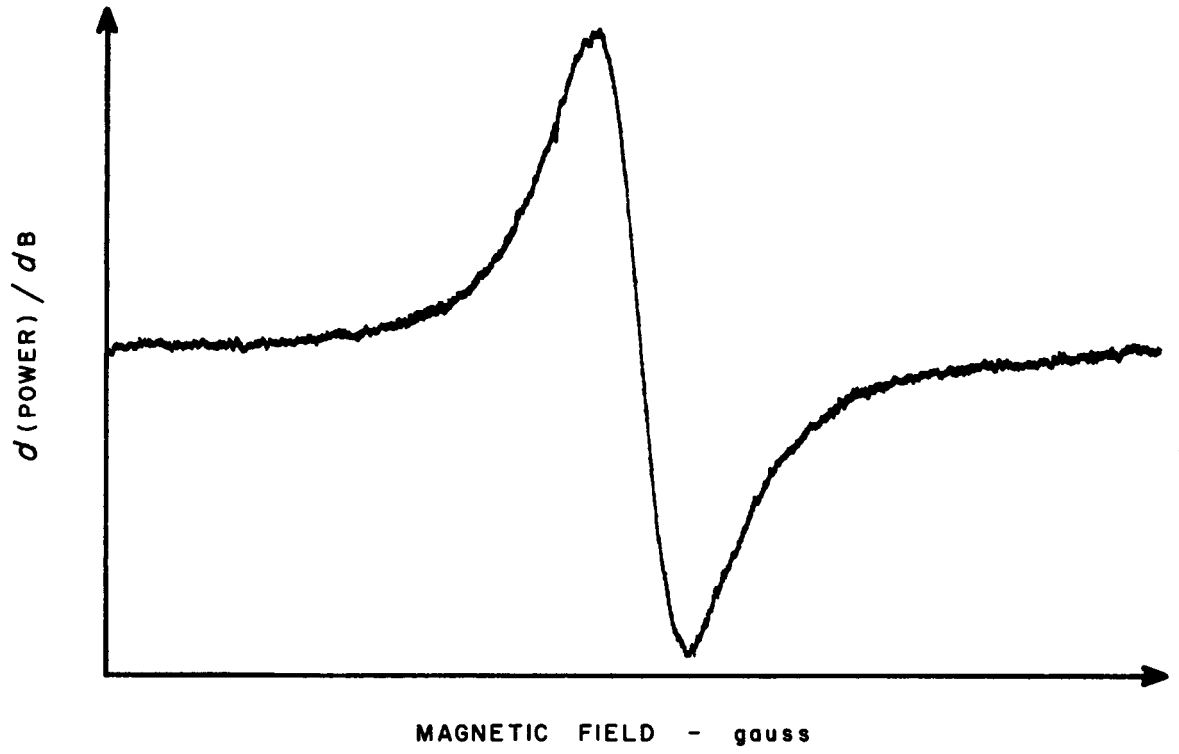

FIG. IB

ILLUSTRATION OF SPECTRAL WIDTHS

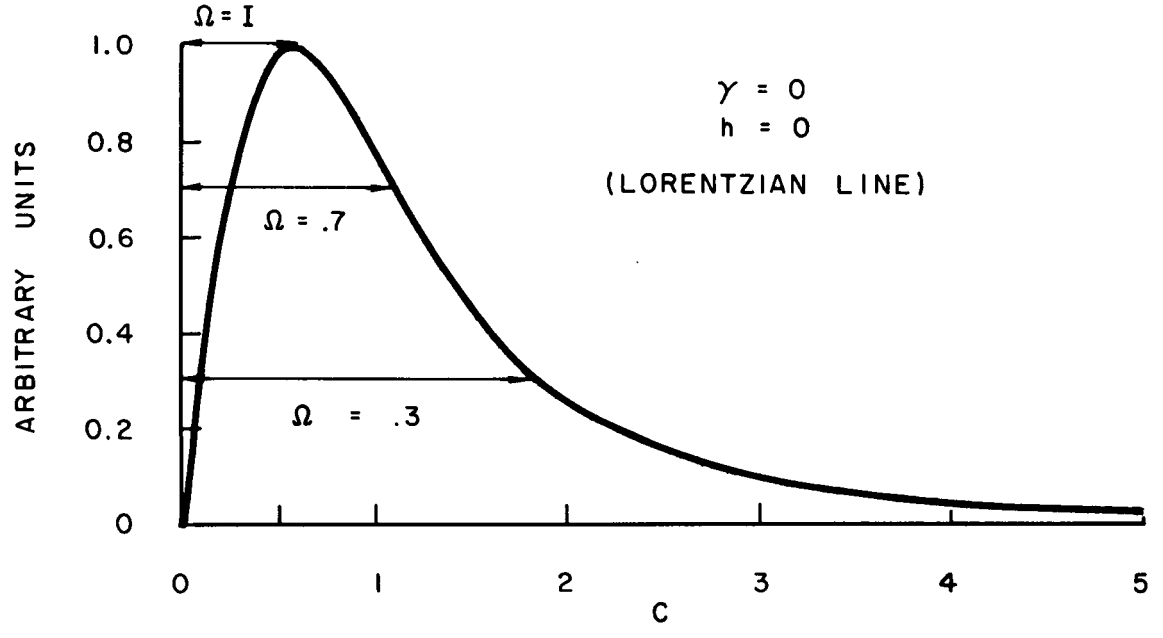

FIG. 2

SOLUTION OF EQUATION 4

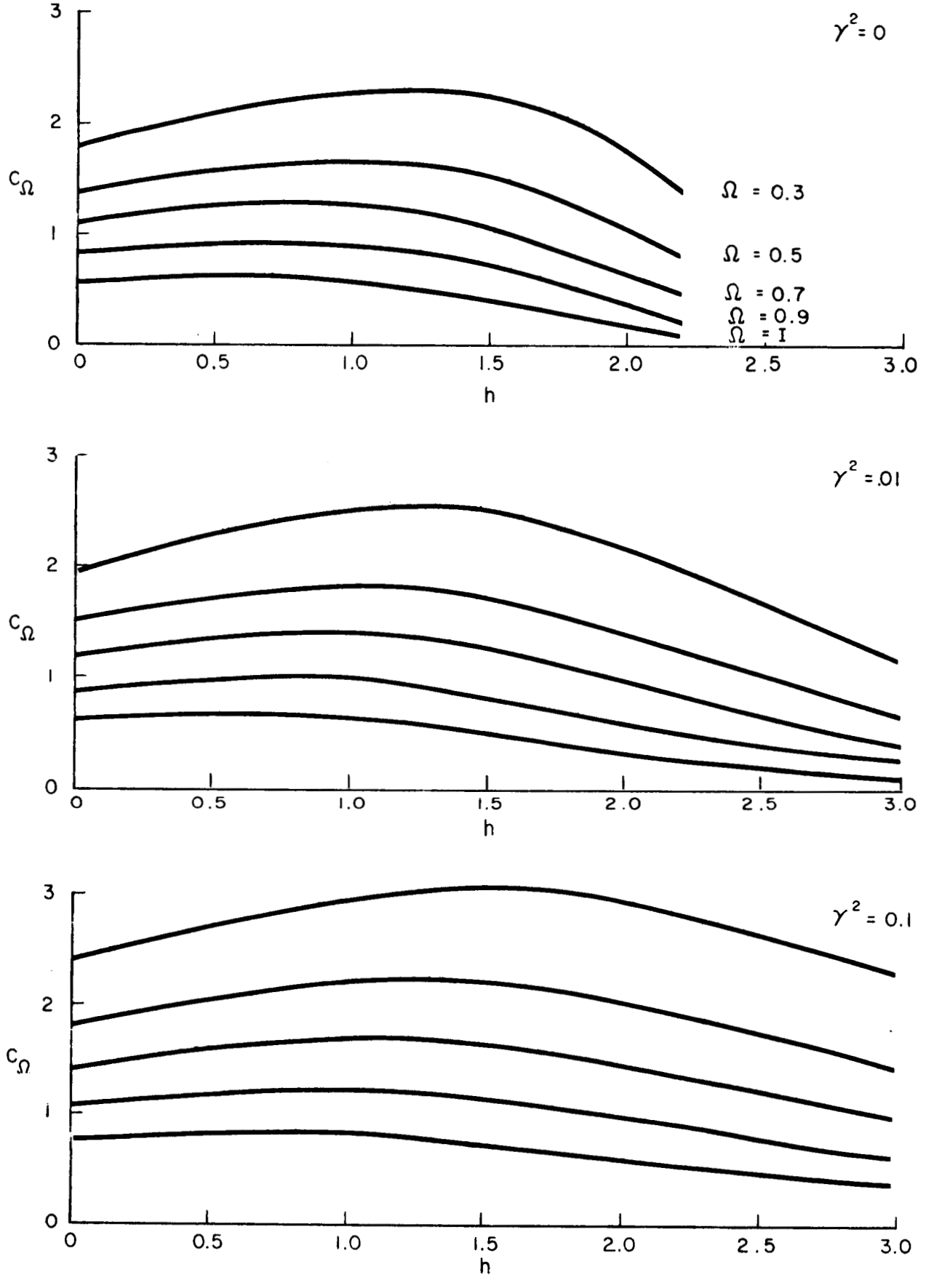

A-920057-5

FIG.3

CALCULATED RATIO OF SPECTRAL LINE WIDTHS

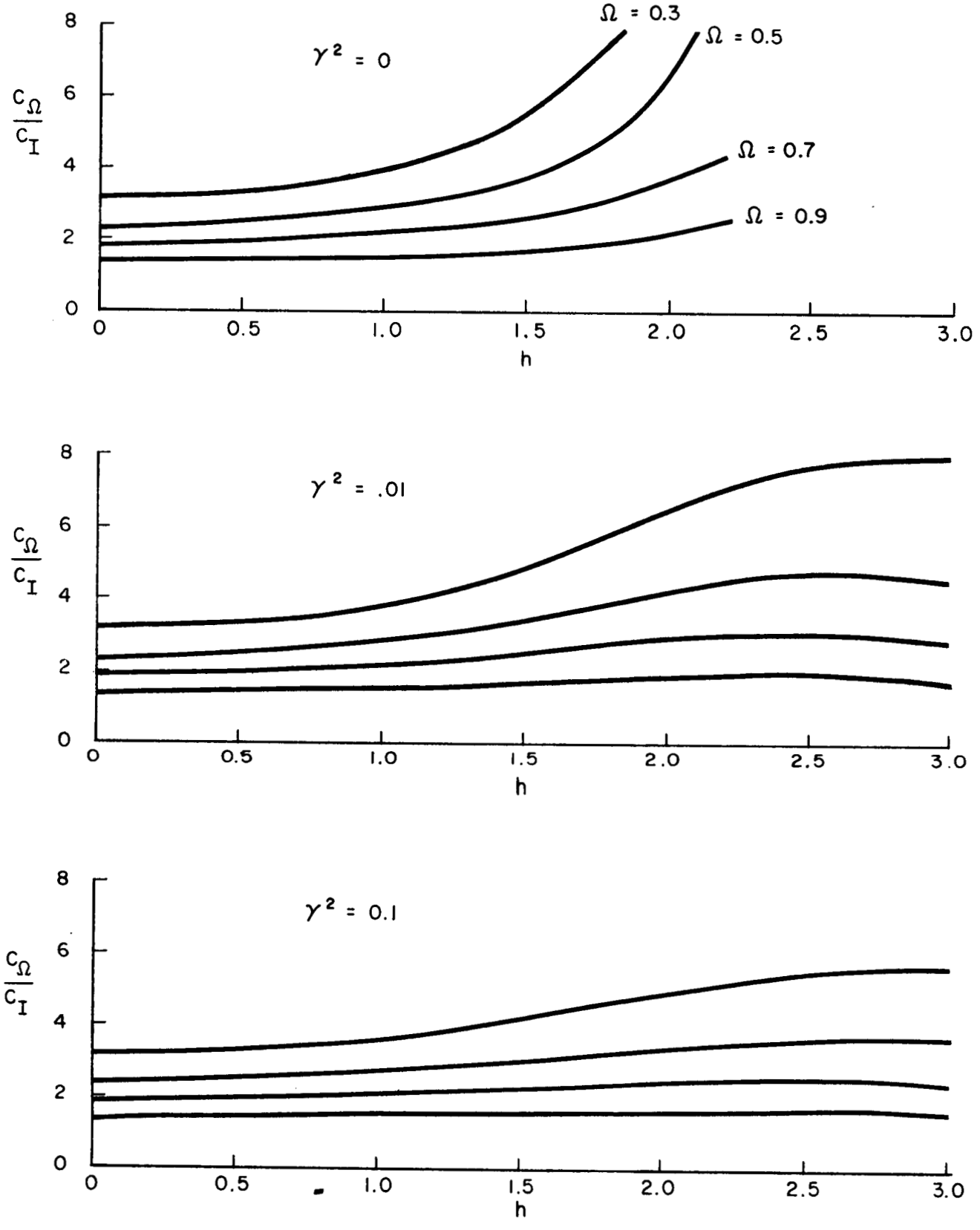

A-920057-5

FIG. 4

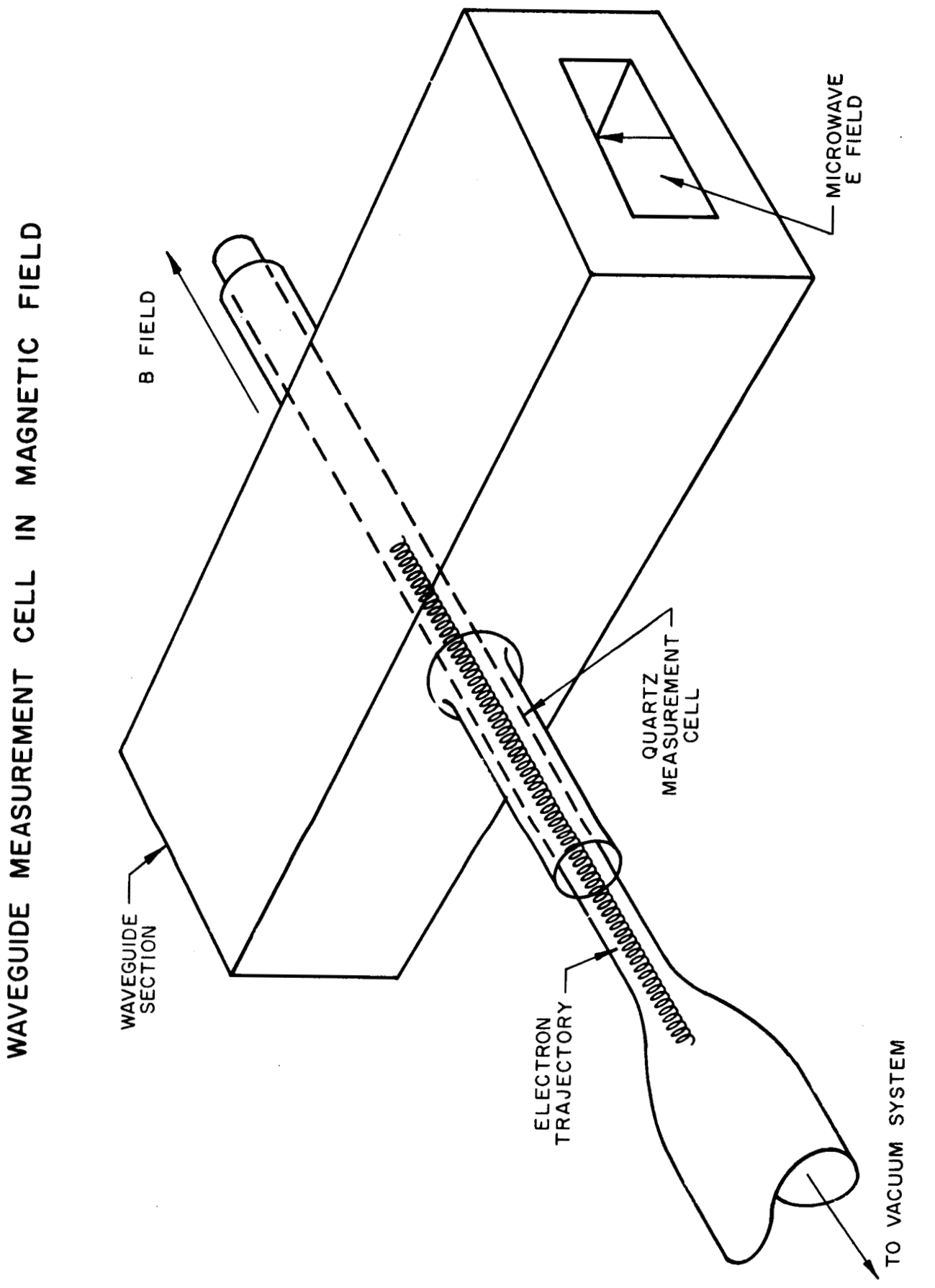

FIG. 5

MICROWAVE SPECTROMETER

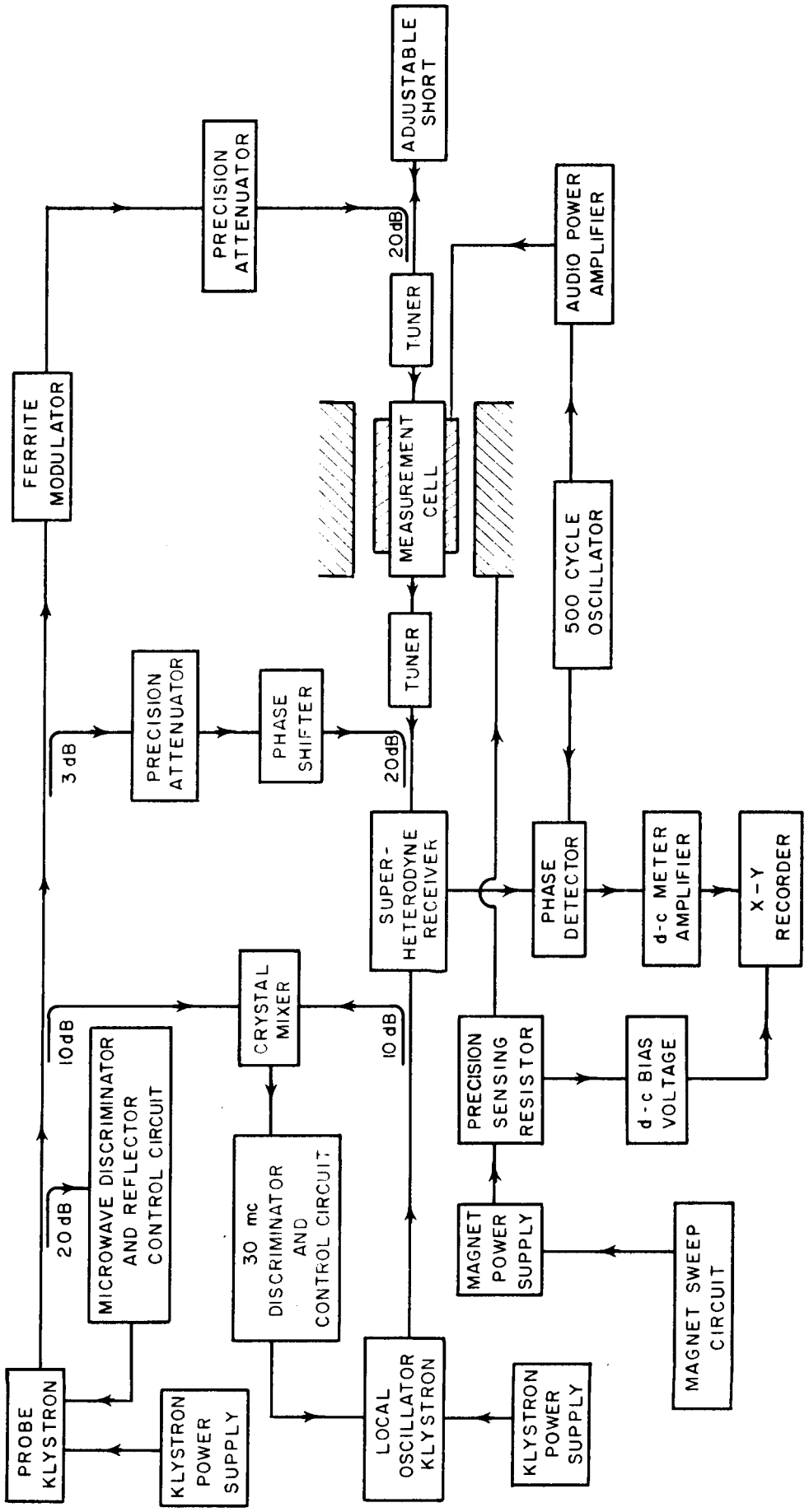

A-920057-5

FIG. 6

DOUBLE OVEN FOR CONTROL OF VAPOR PRESSURE AND ELECTRON ENERGY

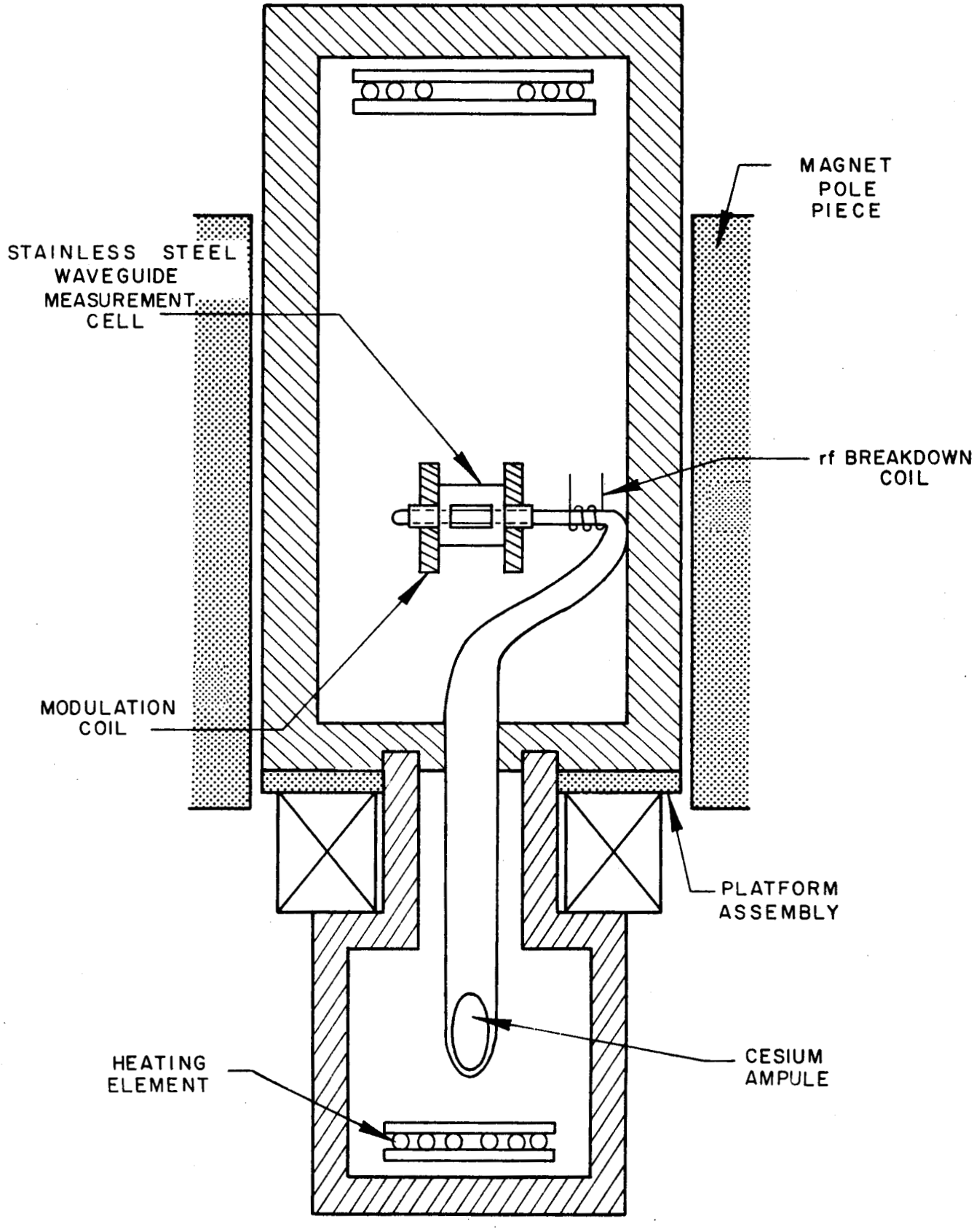

FIG. 7

TECHNIQUE FOR HEATING WAVEGUIDE CELL TEMPERATURE TO 1150 °K

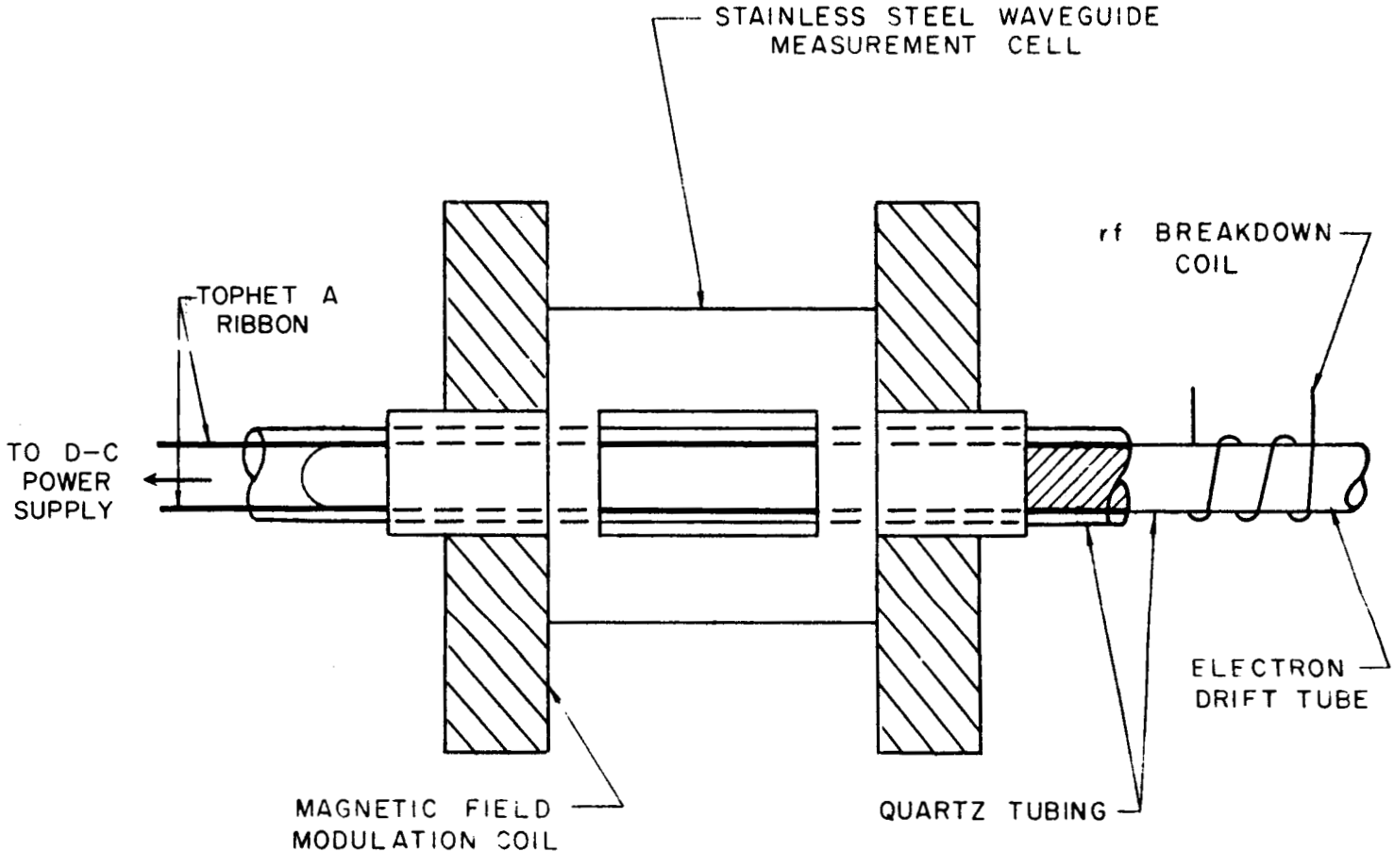

FIG.8,9

LINE WIDTH VS INPUT MICROWAVE POWER

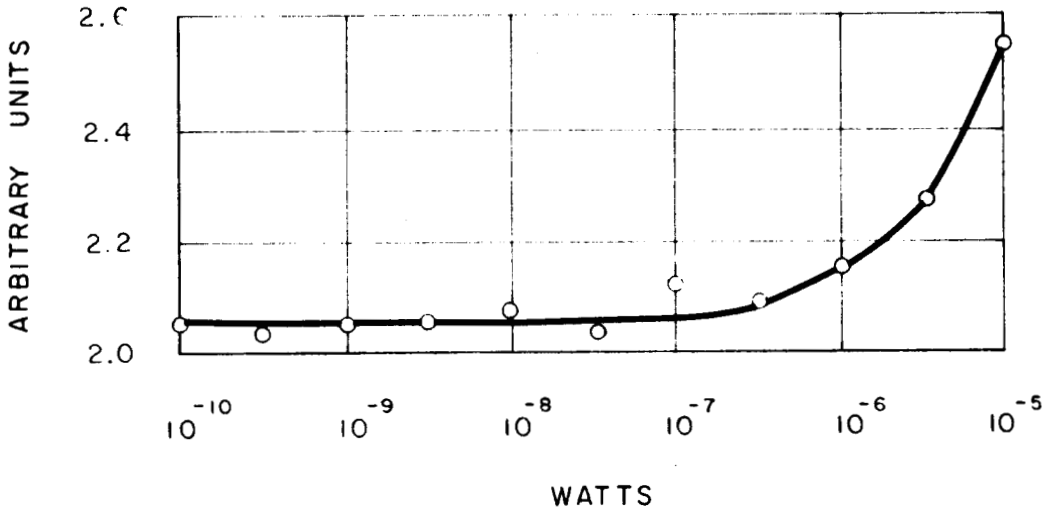

LINE WIDTH VS MODULATION LEVEL

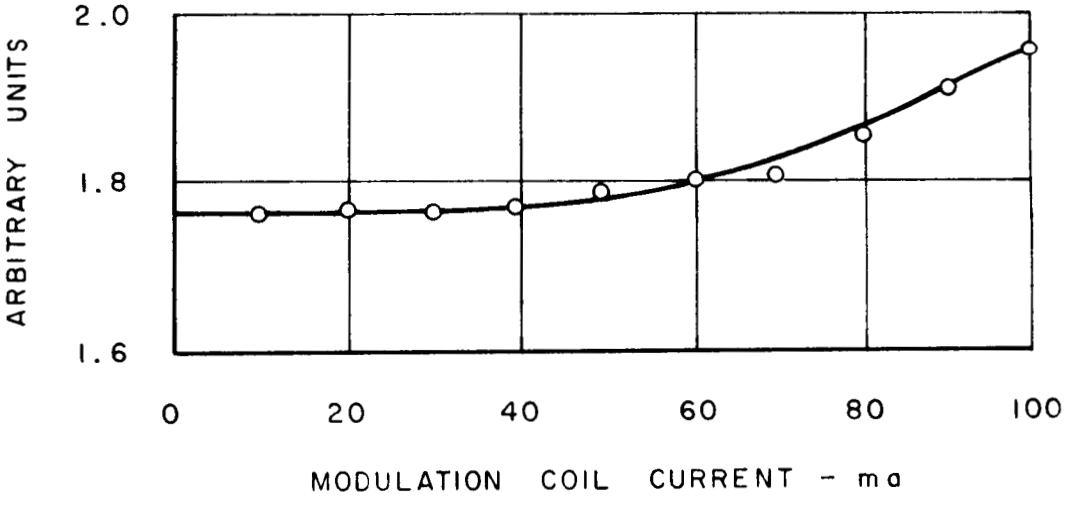

A-920057-5

FIG. 10

DEPENDENCE OF LINE WIDTHS ON PRESSURE

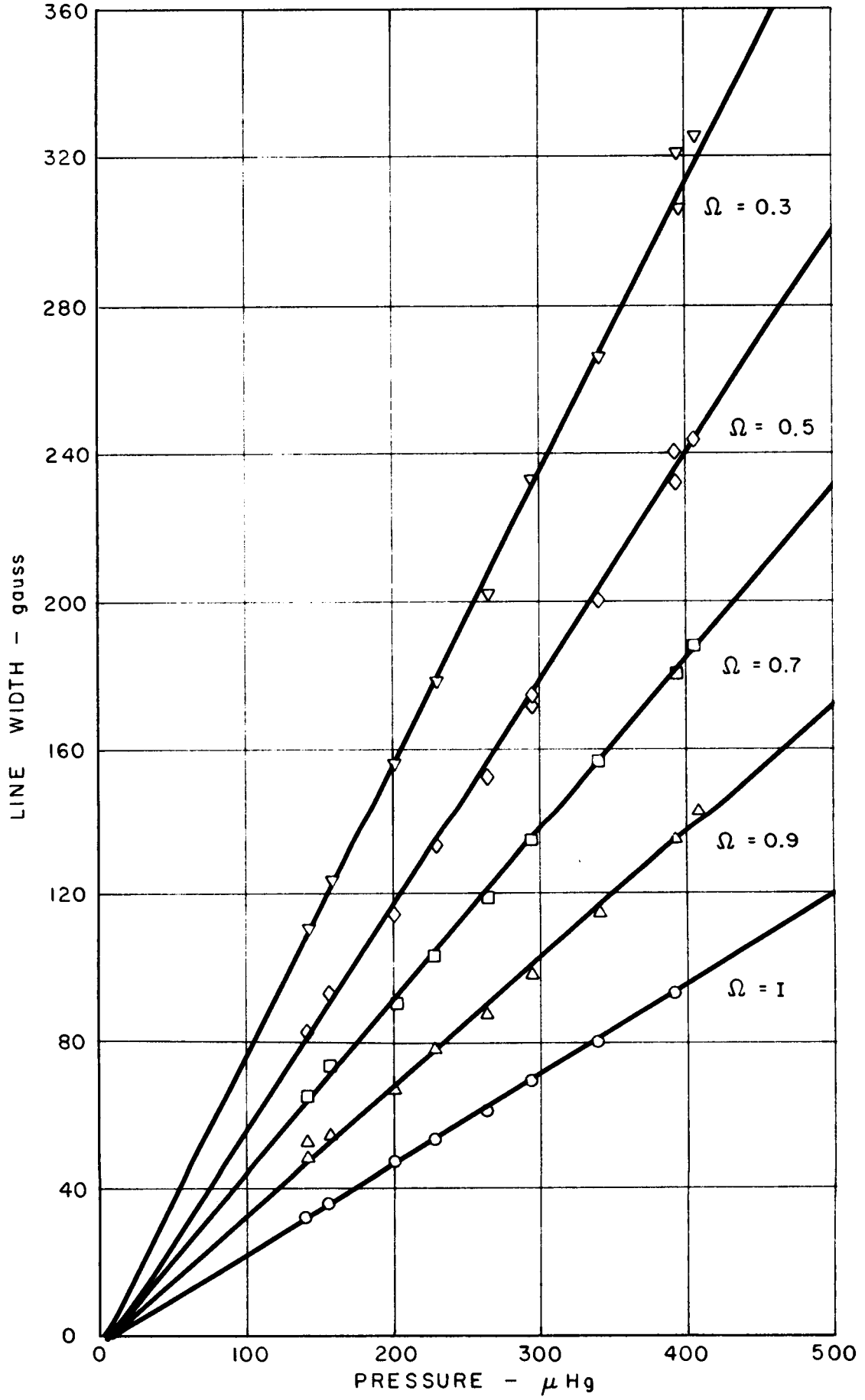

FIG. 11

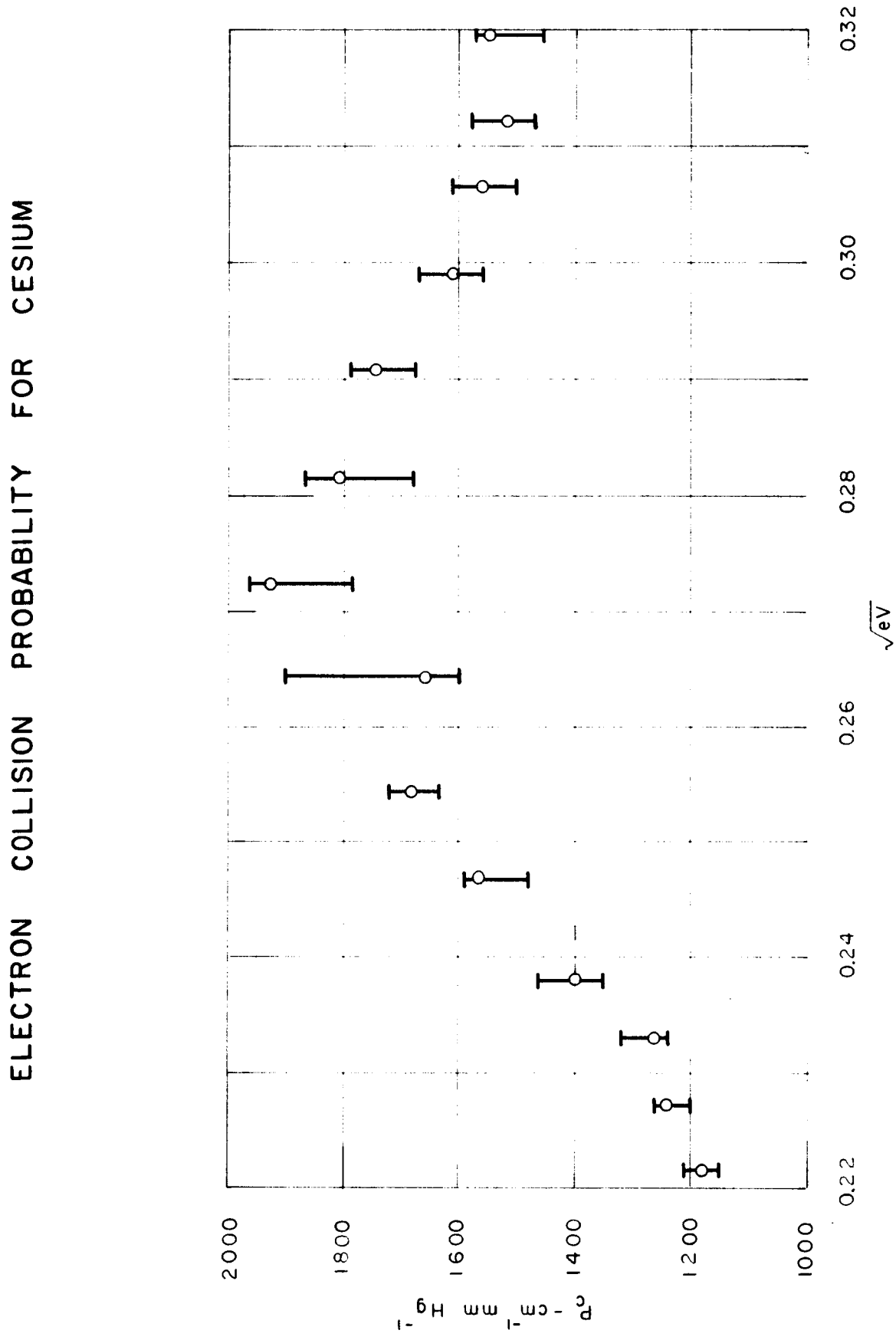
ELECTRON COLLISION PROBABILITY FOR CESIUM
P_c - cm^{-1} mm Hg^{-1}
2000
1800
1600
1400
1200
1000
0.22
0.24
0.26
0.28
0.30
0.32
$\sqrt{eV}$

FIG.12

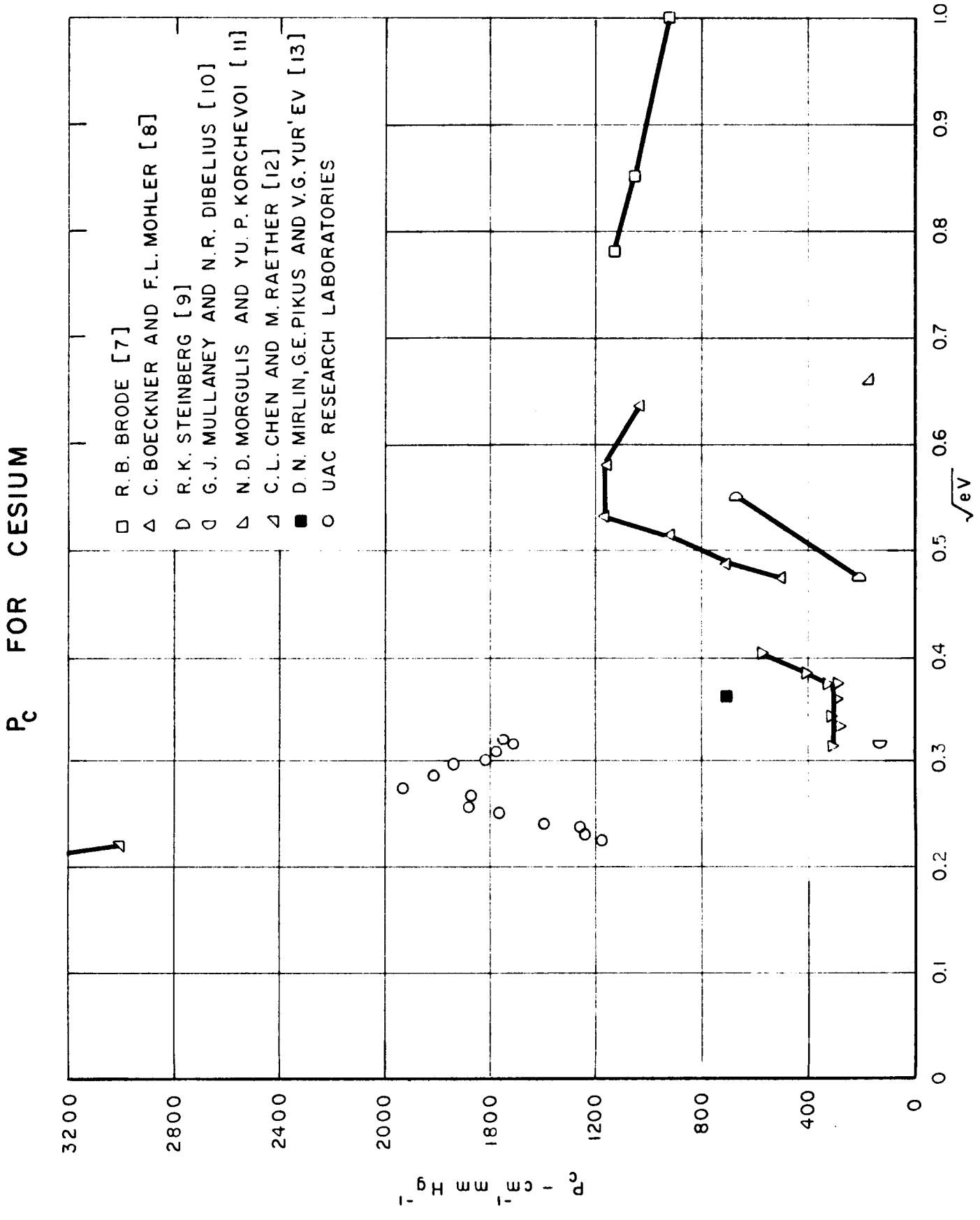
P_c FOR CESIUM
□ R.B. BRODE [7]
△ C. BOECKNER AND F.L. MOHLER [8]
D R.K. STEINBERG [9]
◁ G.J. MULLANEY AND N.R. DIBELIUS [10]
△ N.D. MORGULIS AND YU. P. KORCHEVOI [11]
◁ C.L. CHEN AND M. RAETHER [12]
■ D.N. MIRLIN, G.E. PIKUS AND V.G. YUR'EV [13]
○ UAC RESEARCH LABORATORIES
P_c - cm^{-1} mm Hg^{-1}
3200
2800
2400
2000
1800
1200
800
400
0
0
0.1
0.2
0.3
0.4
0.5
0.6
0.7
0.8
0.9
1.0
$\sqrt{eV}$

ION COLLISION CROSS-SECTION MEASUREMENTS

Introduction

The total cross section for collisions of cesium ions with cesium atoms has been measured with a modified Ramsauer Experiment in which contact potential differences have been eliminated in the collision chamber. For energies less than 1 ev, small stray electric fields of the order of millivolts per cm can drastically effect ion trajectories giving rise to spurious experimental results. The basic design concept used in this experiment is to produce a completely field free region in which the energy of the ion beam can be uniquely determined and in which the collisions can take place. With this design it is not necessary to accurately know ion beam energies before the particles enter or after they leave the collision chamber. However, while the cesium ion is within the collision chamber interacting with cesium atoms its energy is uniquely known since the radius of curvature which it is forced to follow in the magnetic field is defined by the geometry of the chamber. This technique also eliminates errors which may occur when the particle energy is determined by measuring applied potentials which can be in serious disagreement with electrode surface potentials in cesium environments.

Experimental Configuration

A schematic of the ion cross section experiment is shown in Figure 1. Ions are generated by contact ionizing cesium atoms which flow through a hot porous tungsten cap. The ions produced at the hot tungsten cap are accelerated and focused by a series of slits in front of the source. The ions then travel on a curved path determined by a homogeneous magnetic field generated by Helmholtz coils and enter the small slits in the collision chamber.

The collision chamber which will be described in detail in a following section has two re-entrant slits so that electric fields generated in other sections of the experiment will not effect the ion radius of curvature inside the chamber. If the ion has the proper energy, it will pass through the three points of geometrical constraint within the chamber and emerge from the exit slit. This chamber is arranged so that it can be filled with cesium vapor, without introducing perturbing electric fields. Ions of the proper energy to traverse the chamber which suffer collisions

are deflected from the beam and are collected on the walls. Collisions within the chamber result in an attenuation of the ion beam emerging from the chamber which was collected either by a Faraday cup or an ion multiplier.

Ion Source

The ion source assembly is shown in Fig. 2. The entire assembly is mounted on a metal flange with ceramic terminals that provide electric isolation for support rods and electrical leads required to apply potentials within the source. Liquid cesium is contained within a boiler heated by a separate heating element at the rear of the source. Cesium flows through a thin walled stainless steel tube feeding the ionizer which consists of a porous tungsten disk, an electrical heater, and heat shields. The electrical heaters are bifilar wound and operate so that the cap is at a temperature of roughly 1300 K. As the cesium passes through the porous tungsten disk,it is ionized by contact ionization on the disk surface. The ion beam formed at this surface is extracted by focusing electrodes at the front of the disk. The potentials on the accelerating and focusing electrodes are normally maintained in a manner such that a large negative well of the order of a few hundred volts exists immediately in front of the source. Ions born at the porous tungsten cap are extracted from the surface by this potential well and are then decelerated by succeeding slits until they reach the desired low energy suitable for collision cross-section measurements. Misalignment of the ion source cap with respect to the collision chamber slits was corrected for by the use of deflection plates placed in front of the last focusing plate of the gun and directly in front of the collision chamber.

Collision Chamber Design

The collision chamber was designed to perform two functions. First, it provided three points of geometrical constraint which serve to define the radius of the circle on which the ions travel as they pass through the chamber. This constraint is necessary so that the energy of the ions traversing the chamber may be determined uniquely by the strength of the applied magnetic field. Secondly, the chamber provides a region in which cesium vapor at a known pressure could be introduced in a region that is completely field free so that ion collision cross-section measurements at extremely low energies could be conducted. To prevent electric

fields generated in the rest of the apparatus from penetrating into the chamber, the region immediately adjacent to the slits through which the ions enter and exit was made re-entrant. It was found by measurements on electrically conducting paper that the re-entrant design employed was one of the few designs which prevented the penetration of electrical fields into the chamber.

Since contact potentials within the chamber can seriously perturb the trajectories of low energy ions, the collision chamber had to be fabricated so that metal interfaces or other possible areas of contact potentials were completely eliminated. A uniform metal surface without interfaces and with the intricate shape required for the collision chamber was fabricated by plating an aluminum mandrel to a thickness of 0.050 inches with pure copper in a plating bath without additives. The mandrel was then removed by chemical etching with caustic solutions which only attacked the aluminum. Since additives were eliminated from the plating bath and only high purity electrodes were used in this process, the resulting electroformed collision chamber was found to be of high purity and exhibited excellent vacuum characteristics, even at elevated temperatures.

A photograph of an electroformed collision chamber is shown in Fig. 3. Two ports which provide cesium to either end of the collision chamber between the middle constraint point are visible pointing upward in the figure. The view is looking directly into one of the slits which is positioned in the center of one of the re-entrant surfaces of the collision chamber. The thickness of the collision chamber walls, the re-entrant slits and the center constraining section are shown in an x-ray of this collision chamber in Fig. 4. The x-ray was also used to determine that there was absolutely no aluminum from the mandrel left in the chamber after etching.

Ion Detecting System

Either a Faraday cup type collector or a twenty stage electron multiplier was used to measure ion beam currents exiting the collision chamber. The electron multiplier was positioned off the axis of the ion beam trajectory as shown in Fig. 1 and an acceleration plate was used to deflect the ions into the first dynode of the multiplier. A photograph of the twenty stage electron multiplier which was used to provide the required increased sensitivity is shown in Fig. 5. The multiplier was used at current levels below 10^{-12} amps at which point the problem of obtaining high vacuum electrical leads with sufficiently high impedance to measure this extremely low current becomes troublesome. The electron multiplier operates completely

within the vacuum system and provides a current gain of the order of 10^5 to 10^6. This gain results in sufficiently large currents so that ceramic, high vacuum electrical terminals may be used with a minimum of difficulty.

The electron multiplier was constructed by Nuclide Analysis Associates and has been used for an extended period in a cesium environment without serious degradation of the gain. The dynodes are constructed of beryllium copper which has a modest secondary electron emission and good stability over long periods of time.

Vacuum System Design

The vacuum chamber is a stainless steel tank with all flanges being sealed either with gold or copper O-rings. Electrical connections are made to the chamber by means of ceramic cable end seals which are welded into metal flanges. Cold traps have been provided in the area adjacent to the cesium ion gun and in the ion multiplier to reduce the cesium vapor pressure on these critical points. Control of the collision chamber and cesium reservoir temperatures are maintained independently by pumping heated Dow 550 heat transfer oil to each chamber. The collision chamber slit size has been determined so that at the maximum pressures in the chamber only one gram per hour of cesium will be lost through the slits. The chamber containing the cesium ion source is completely isolated from the chamber containing the ion multiplier by a ceramic disk which supports the collision chamber and electrically insulates it from ground potential. Placing the ion source which ejects a copious quantity of cesium ions and electrons as well as neutral cesium atoms in a separate vacuum environment from that of the Faraday cup and the ion multiplier was found to be essential to obtain low noise levels.

Complete System

The overall system is shown in Fig. 6. The collision chamber is inside the stainless steel vacuum tank at the left of the photograph. The three large pancake coils on the top of the chamber are one half of the Helmholtz coil which provides the uniform magnetic field for ion energy analysis. The equipment to regulate and measure the potentials applied to the slits of the gun, the electron multiplier and the deflecting plates are in a rack to the right of the apparatus.

System Performance

Fig. 7 shows a typical ion energy distribution obtained with the ion source and electroformed collision chamber. The resolution at this low energy represents good energy selection of the ions. Proper adjustment of all focus electrodes as well as the deflect plates to properly position the ion beam on the radius of the collision chamber was found necessary to obtain high current ion beams. The measured ion current passing through the collision chamber as a function of the ion energy is shown Fig. 8. Preliminary measurements to verify ion source operation had been made previously with a dummy collision chamber substituted for the electroformed chamber. In the construction of this dummy chamber no attempt was made to eliminate contact potentials. It was found in the course of the experiments that the minimum energy at which a detectable ion beam could be focused through the system decreased significantly with the use of the electroformed chamber. At an energy of 0.1 ev current of the order of 6×10^{-18} amps has been measured with the electroformed chamber in the system. Although this current is extremely low it is entirely satisfactory for use in experiments to determine collision cross sections and verifies the soundness of the original experimental concept. The deviation from the space-charge current limited curve is quite interesting. It is felt that this deviation occurs at ion energies at which the velocity of the ions perpendicular to the beam is comparable to the directed velocity. The perpendicular velocity leads to beam spreading and a reduction of beam current.

At higher energies, the current from the source is predicted quite well by the space charge limited current relationships. Figure 9 shows the performance of this system at low current levels. The difference between the noise level and the reading of 2×10^{-18} amps should be noted as well as the signal due to ion current detected on the 0.1 ev ion peak.

At the low ion current levels it was found necessary to turn off the ion gauge in this part of the vacuum system to reduce the multiplier noise level. Since the ion gauge was isolated from the multiplier in the system by a cold trap and an extremely unfavorable path for ions exists from the gauge to the multiplier, this result seems extremely significant.

Cesium purity used for these measurements was of extreme concern. However, it was found extremely desirable to have small levels of other alkali metals in the cesium in the ionizer gun. By observing the ratio of ion peaks which

appeared in the spectrum it was possible to positively identify the cesium ion beam with relation to the other alkali metal impurities. The cesium used in the collision chamber was supplied by the Dow Chemical Company and their analysis showed a total impurity content of 0.0211 per cent with other alkali metals constituting 0.0068 per cent of this level.

DISCUSSION OF RESULTS

Figure 10 shows ion charge exchange collision cross sections reported in the literature for cesium ions in cesium vapor for ion energies in the range of 5.0 ev to 10 Kev. The present experiment measures the total collision cross section in the energy range of 0.12 to 9.7 ev which is an energy range considerably lower than those previously reported. Therefore, it would be expected that the collision cross sections measured in the present experiment would be higher than the charge exchange cross sections in the literature. Also, it would be expected that the cross section would approach the theoretical limit reported by Sena in Ref. 1.

The pressure measurements made in this experiment were based on the vapor pressure relationship reported by Nottingham in Ref. 7. Throughout all the tests the collision chamber was maintained at a temperature of approximately 430 K which was always higher than the required cesium well temperatures. This was done to maintain a relatively uniform coating of cesium on the inner surfaces of the collision chamber. All reported cross-section information has been corrected for the density difference due to the temperature gradient. With this temperature difference between the cesium well and the collision chamber it has been calculated with information reported in Refs. 8, 9, and 10 that less than 0.05 per cent of the cesium density in the upper chamber is due to molecular cesium.

Shown in Fig. 11 is a typical ion current attenuation due to increasing cesium pressure in the collision chamber. The total collision cross sections presented in Fig. 12 should be considered preliminary with the actual magnitude of the cross section reliable to 20 per cent. In the low energy regime no correction has been made for the velocity of the target (neutral) atoms. This would result in a possible correction to the energy scale of 31 per cent at the lowest energy. With further measurements of the cross section at high energies, the velocity dependence on the cross section can be determined. By changing the gas temperature in the chamber and determining the cross section at different energies, the measured cross sections at the lower energies can be corrected for the velocity of the target atom.

REFERENCES

1. S. C. Brown, Basic Data of Plasma Physics (John Wiley & Sons, New York, 1959), Chap. 2, pp. 36-46.

2. R. C. Speiser and R. H. Vernon, "Cesium Ion-Atom Charge Exchange Scattering," ARS Space Flight Report to the Nation, Oct. 9-15, 1961, New York City.

3. D. K. Chkuaseli, V. D. Nikoleishuili and A. I. Guldamashvili, Izvestiya Akademii Nauk (USSR) (Physics Series) 24, 970, (1960).

4. R. M. Kushnir, B. M. Palyukh and L. A. Sena, Izvestiya Akademii Nauk (USSR) (Physics Series) 23, 995 (1959).

5. A. M. Bukhmeev and Y. F. Bydin, Izvestiya Akademii Nauk (USSR) (Physics Series) 24, 964 (1960).

6. O. B. Firsov, "Theoretical Curve Based on Firsov's Method," J. Exptl. Theoret. Phys. (USSR) 21, 1001 (1951).

7. W. B. Nottingham, M.I.T. Research Laboratory of Electronics, Quarterly Progress Report No. 58, July 15, 1960.

8. E. A. Moelwyn-Hughes, Physical Chemistry, Pergamon Press, (1957), p. 417, 968.

9. G. Herzberg, Molecular Spectra and Molecular Structure, I Spectra of Diatomic Molecules, 2nd ed., van Nostrand, New York (1950).

10. F. Sh. Shifrin, A Method of Investigating the Electronic States of Diatomic Molecules, Doklady, I, 5, 557 (1956).

A-920057-5

FIG. 1

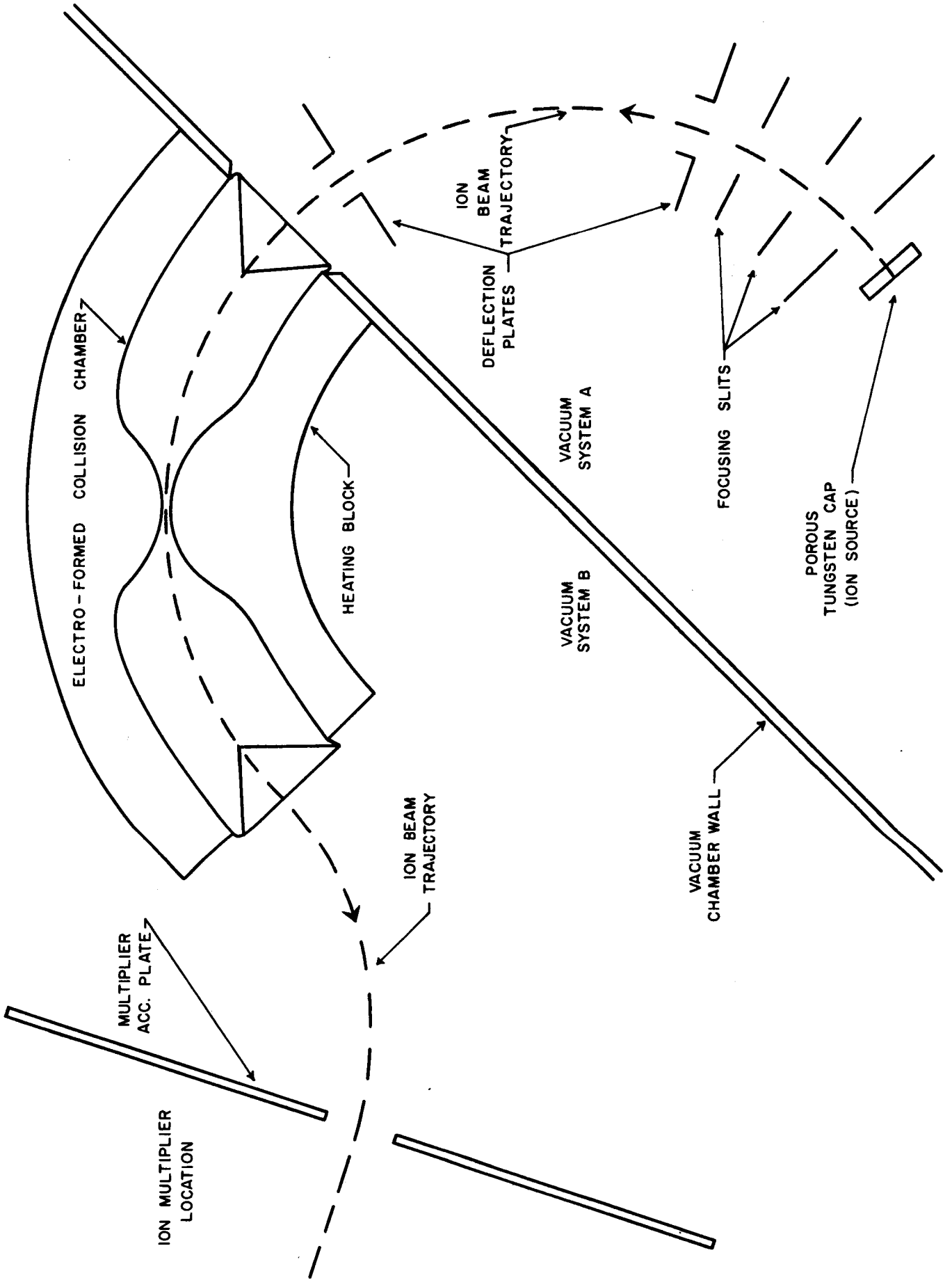

ION SOURCE ASSEMBLY

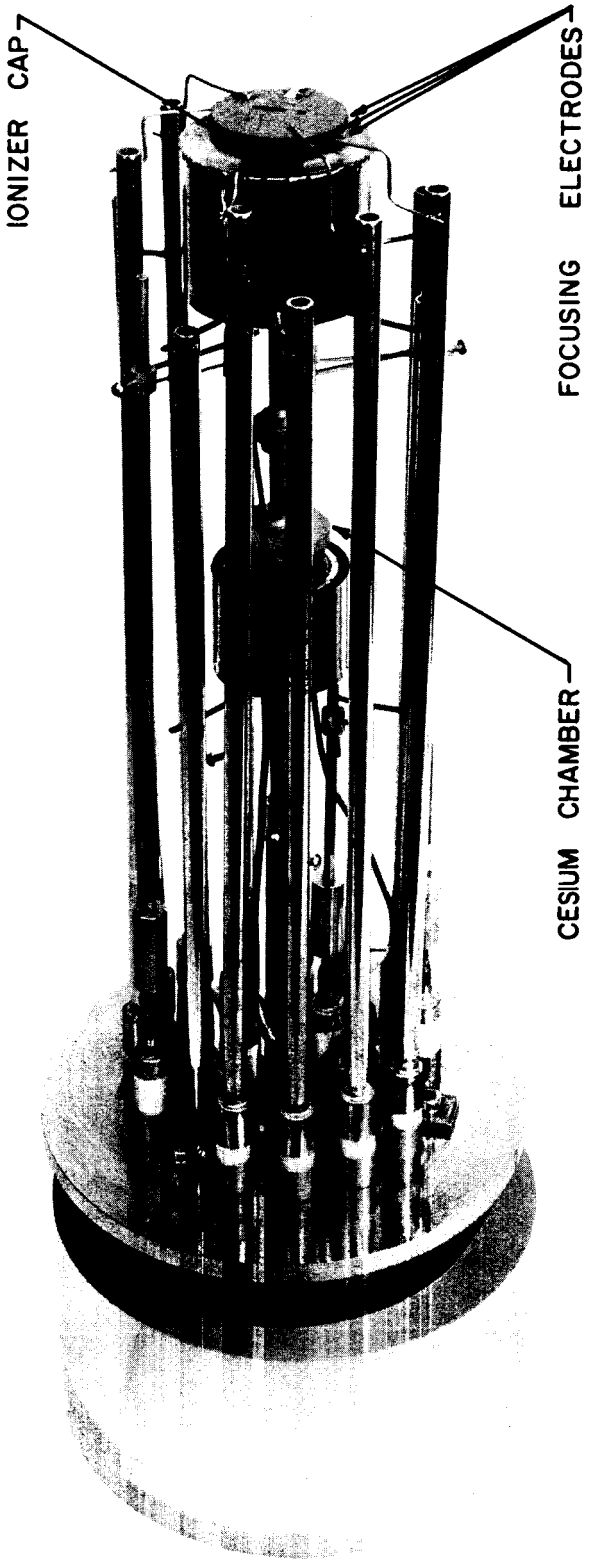

ELECTRO-FORMED COPPER COLLISION CHAMBER

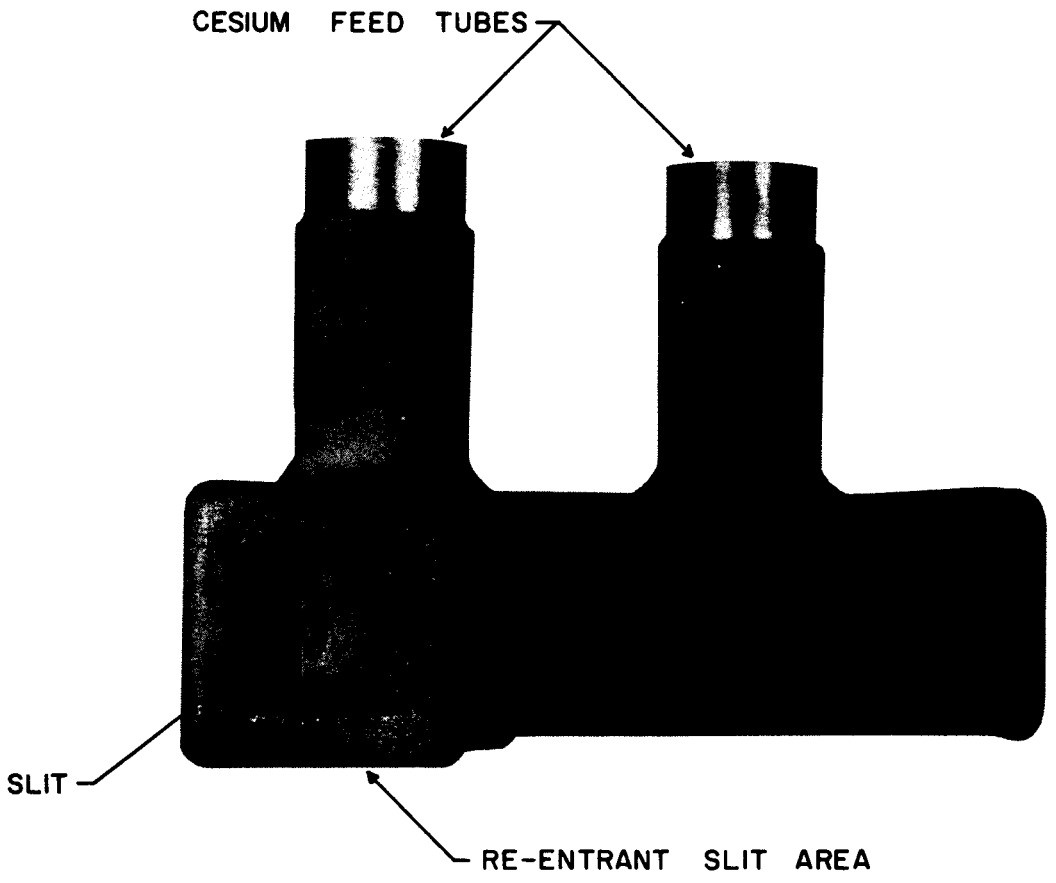

FIG. 4

X-RAY OF ELECTRO-FORMED COLLISION CHAMBER

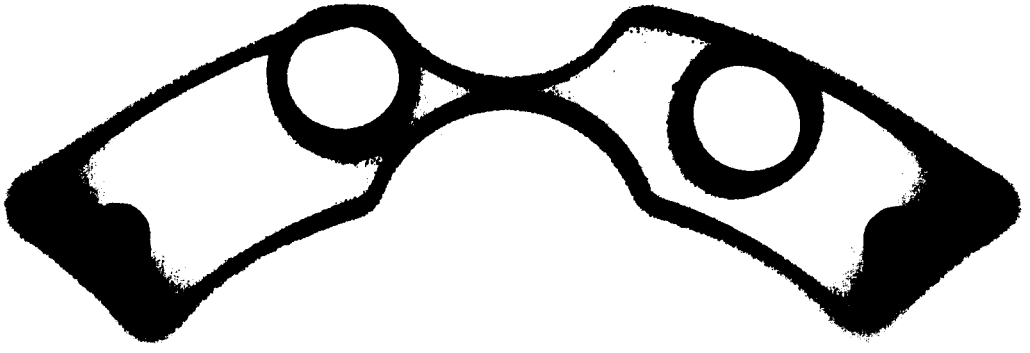

ION MULTIPLIER SYSTEM

20 STAGE DYNODE STRUCTURE WITH DEFLECTION PLATES

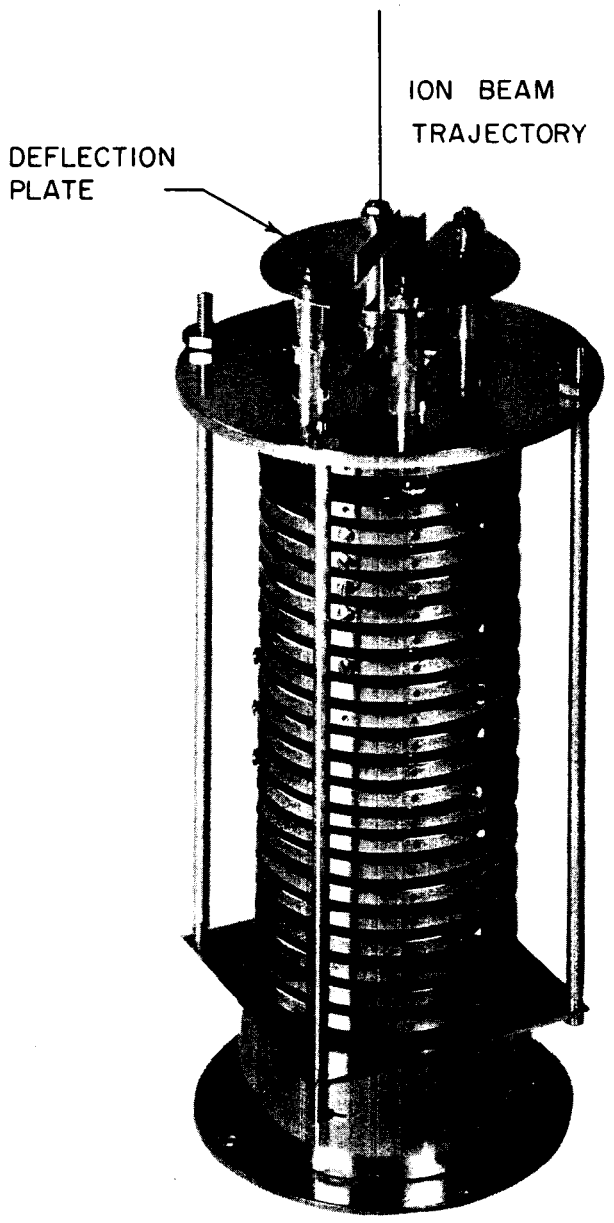

FIG. 6

FINAL ION COLLISION CROSS-SECTION APPARATUS

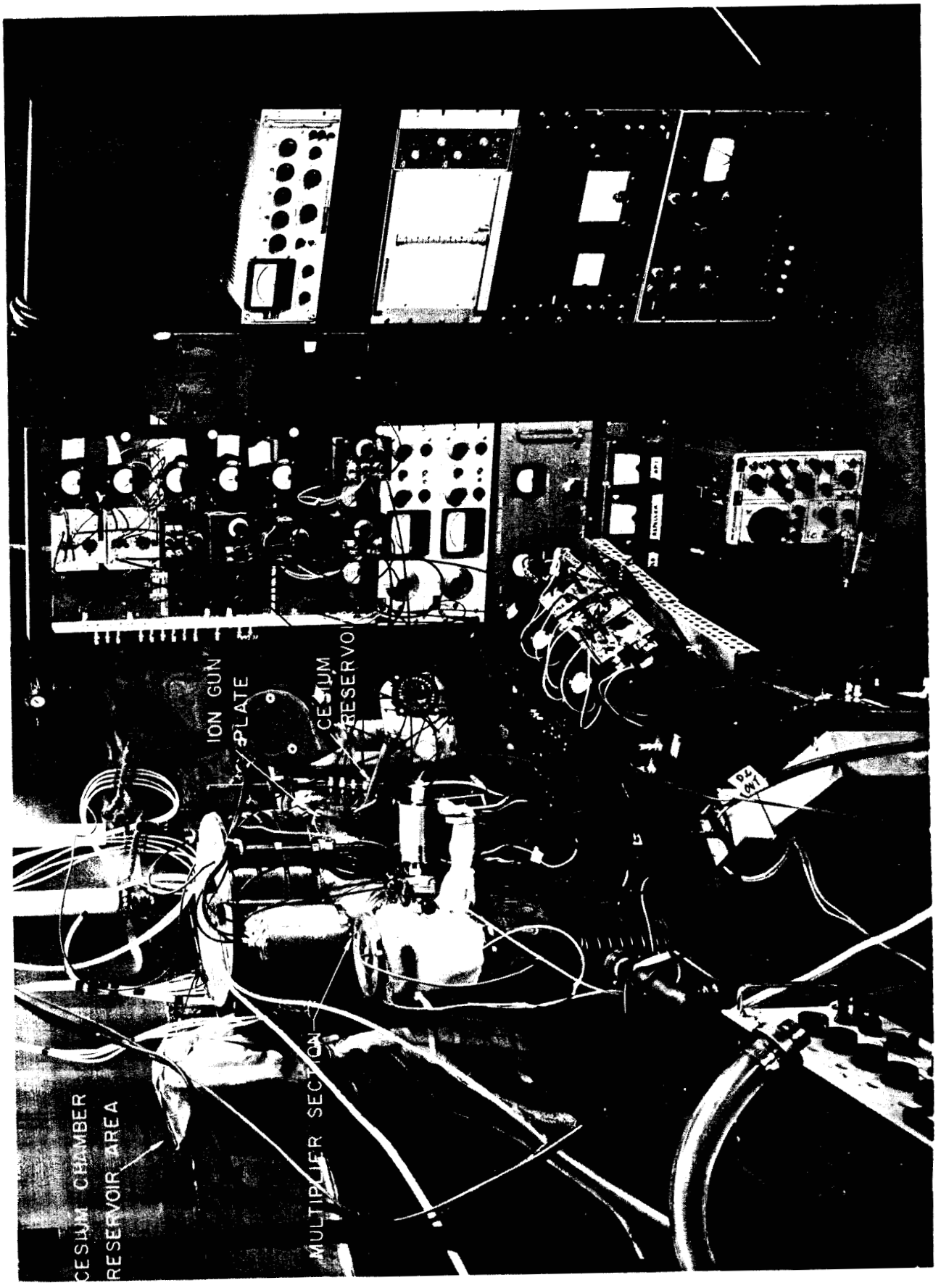

FIG. 7

TYPICAL ION BEAM ENERGY DISTRIBUTION

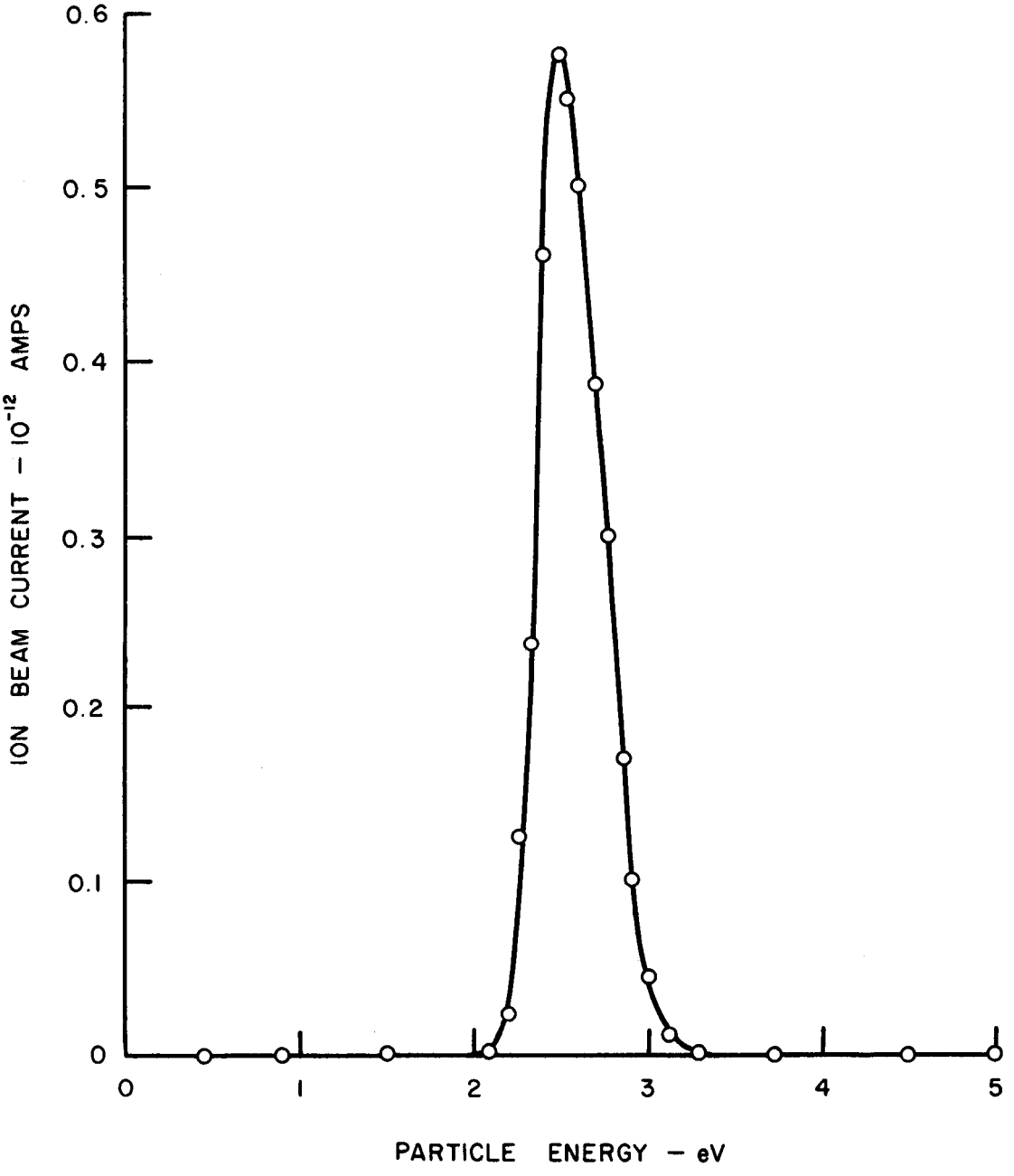

A-920057-5

FIG. 8

LOW ENERGY ION BEAM CURRENT

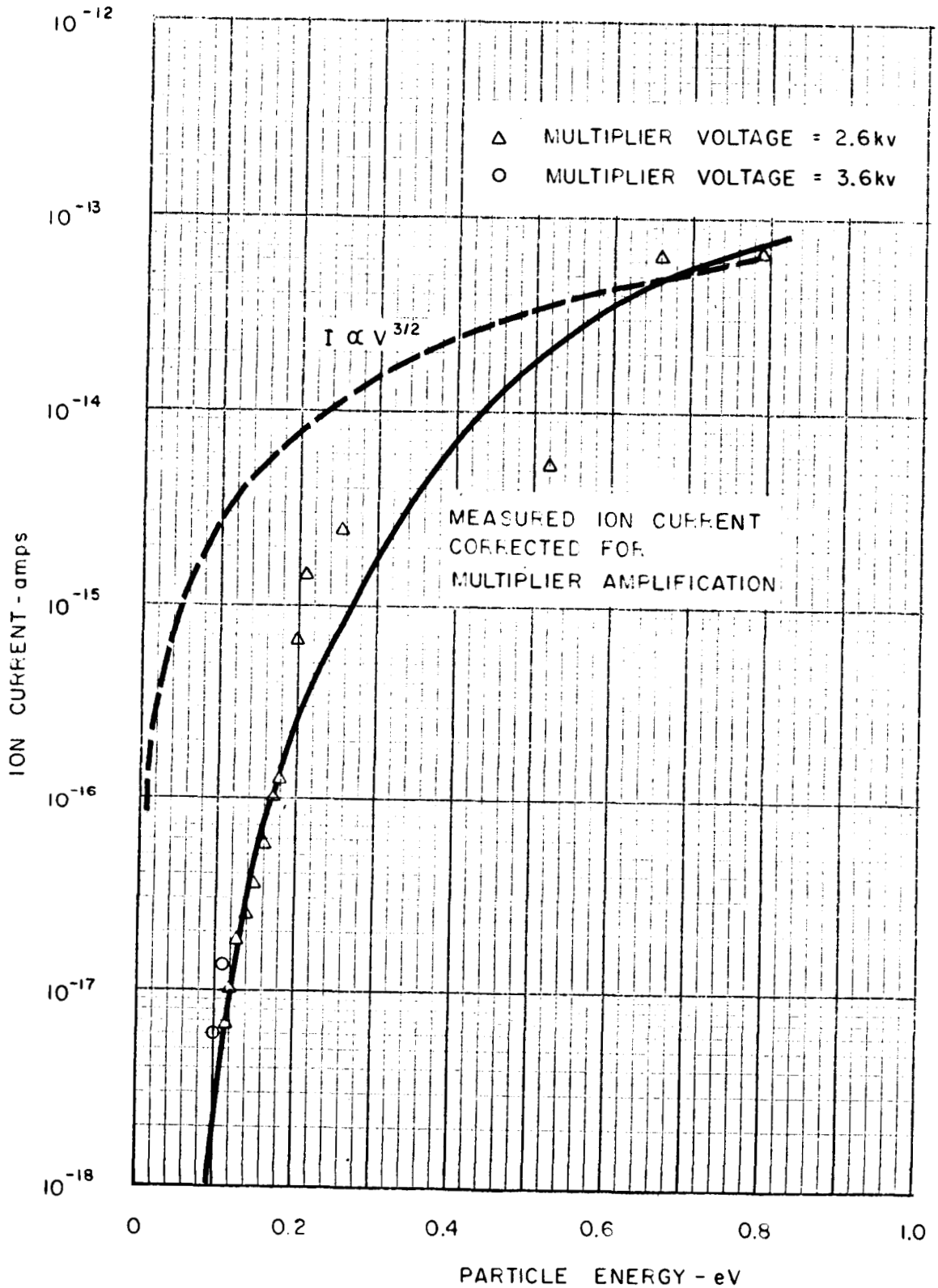

FIG. 9

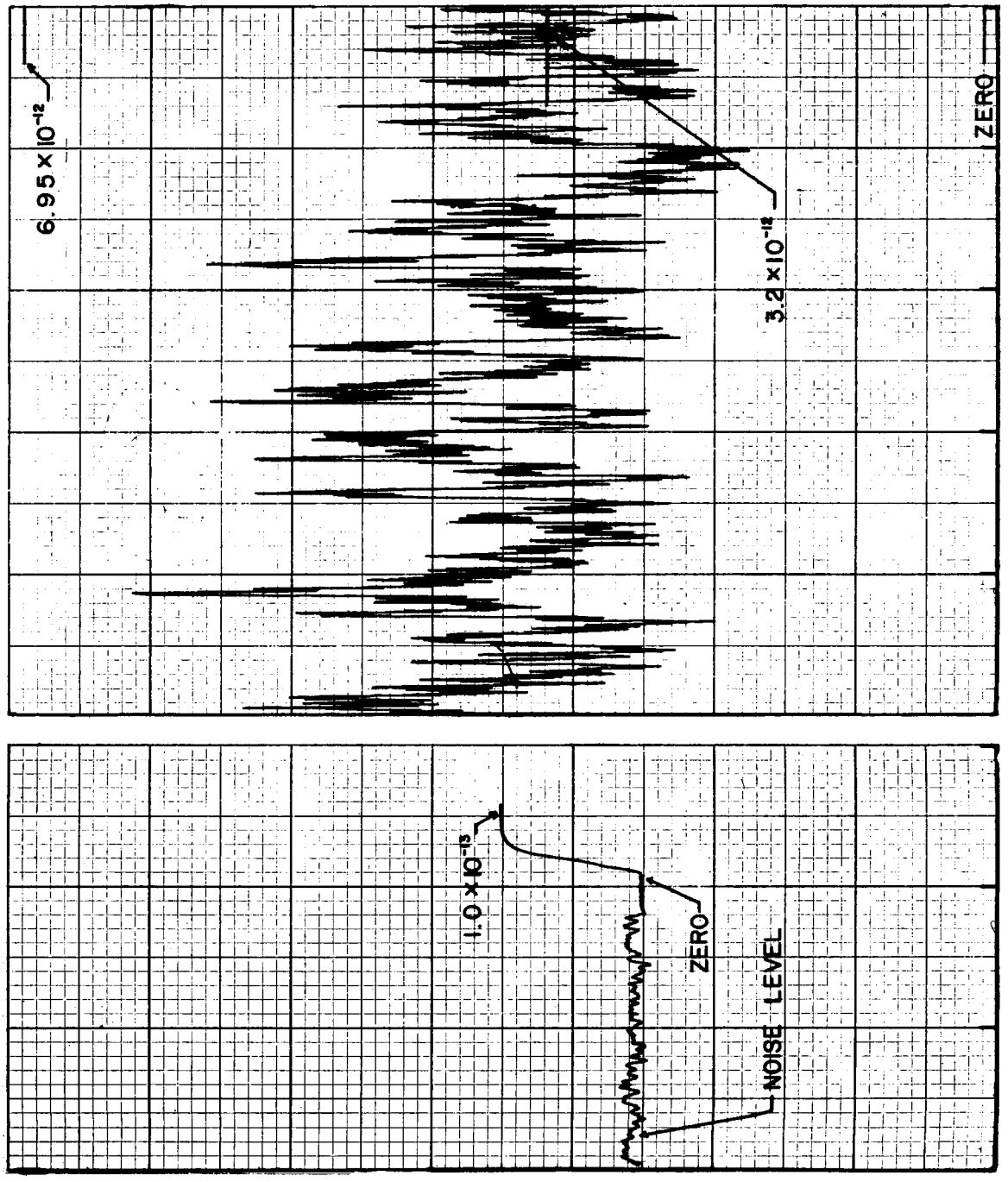
ION BEAM CURRENT AT 0.1 eV
6.95 × 10⁻¹²
3.2 × 10⁻¹²
ZERO
1.0 × 10⁻¹³
ZERO
NOISE LEVEL
AMPS
TIME — 50 SEC/DIV

FIG. 10

REPORTED CHARGE EXCHANGE COLLISION CROSS SECTIONS

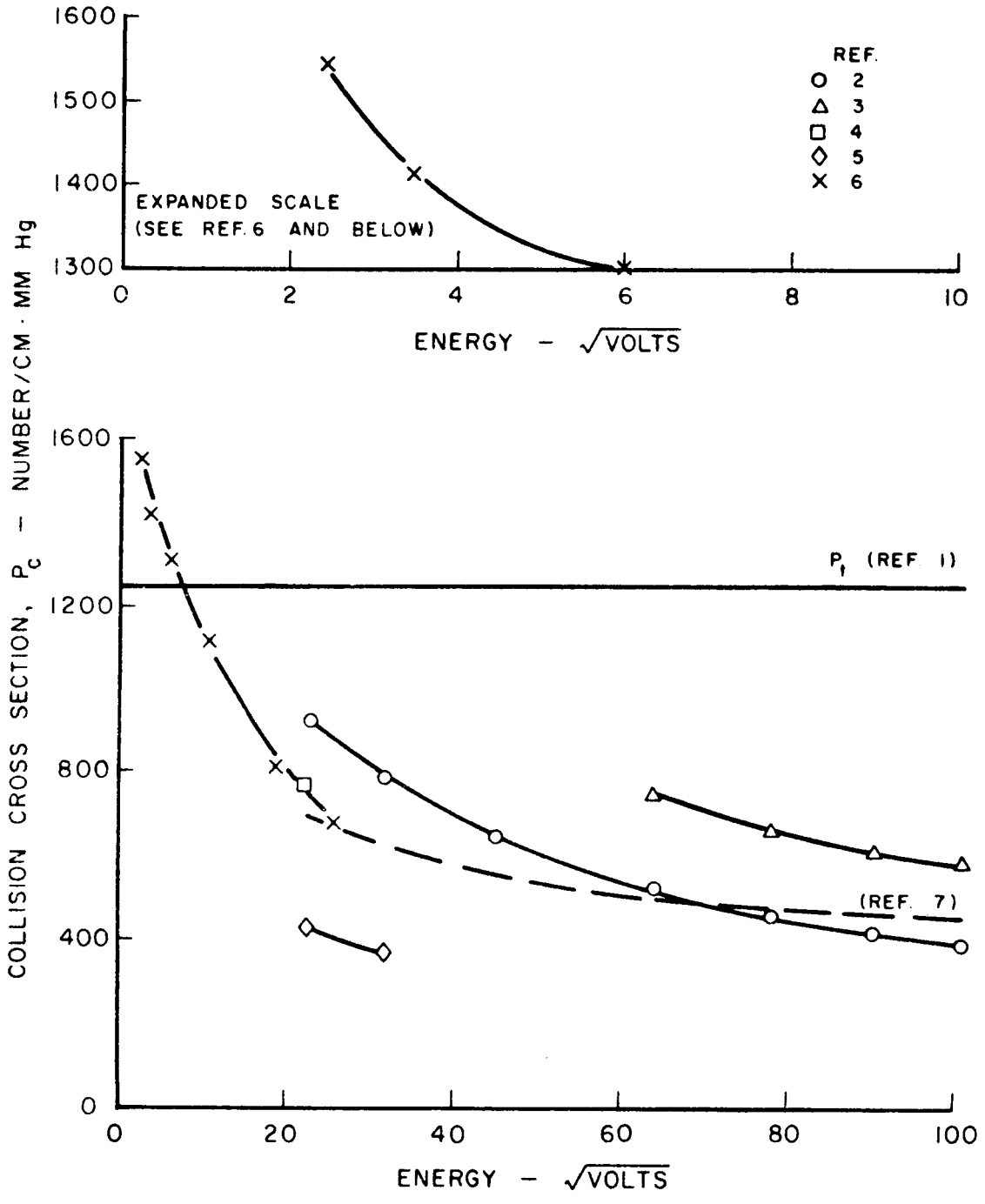

FIG. 11

TYPICAL ION BEAM ATTENUATION WITH INCREASING COLLISION CHAMBER PRESSURE

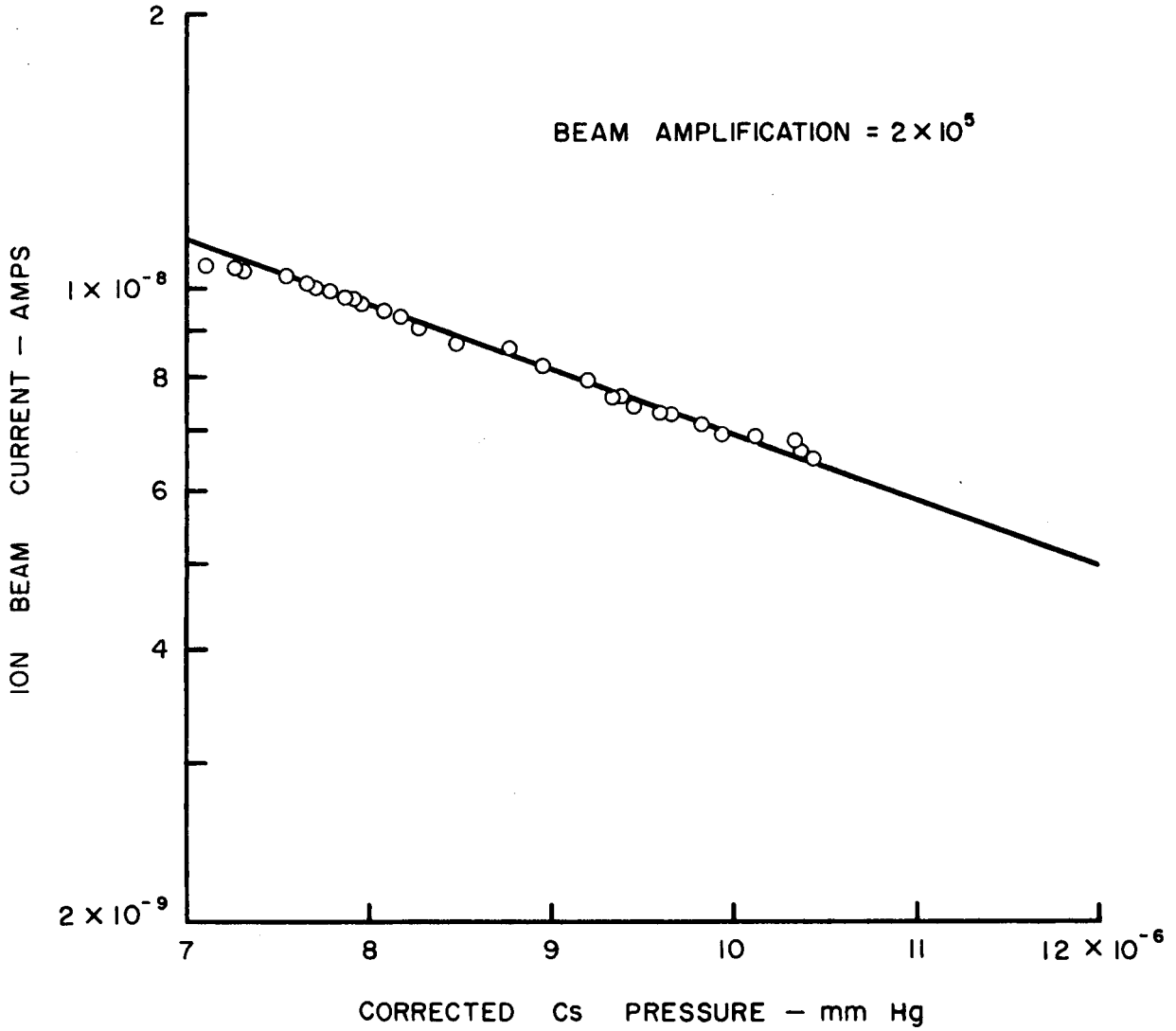

FIG. 12

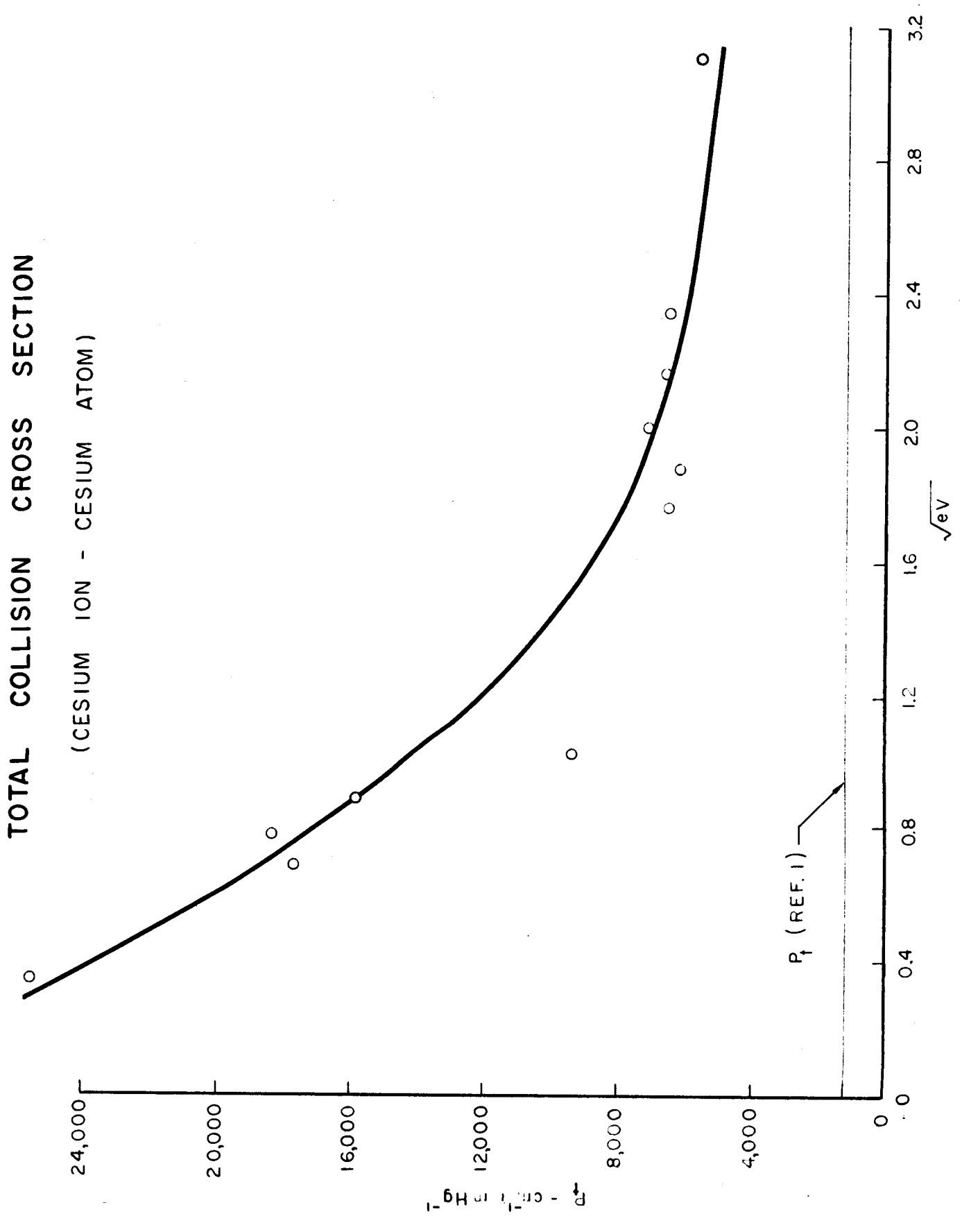
TOTAL COLLISION CROSS SECTION
(CESIUM ION - CESIUM ATOM)
P_t (REF. 1)
24,000
20,000
16,000
12,000
8,000
4,000
0
0.4
0.8
1.2
1.6
2.0
2.4
2.8
3.2
$\sqrt{eV}$